

# Image Shading Taking into Account Relativistic Effects

MENG-CHOU CHANG, FEIPEI LAI and WEI-CHAO CHEN

National Taiwan University

---

This article is concerned with creating more realistic images of 3D scenes which are moving relative to the viewer at such high speeds that the propagation delay of light signals and other relativistic effects can not be neglected. Creating images of 3D scenes in relativistic motion might have important applications to science-fiction films, computer games, and virtual environments. We shall discuss the following problems: (1) how to determine the visual appearance of a rapidly moving object, (2) how to determine the apparent radiance of a scene point on a moving object, (3) how to determine the incident irradiance at a scene point coming from a moving light source, (4) how to determine the color of a rapidly moving object, and (5) how to generate shadows when there are relative motions between the viewer, the scenes, and the light sources. Detailed examples are also given to show the result of shading with the relativistic effects taken into account.

Categories and Subject Descriptors: I.3.7 [**Computer Graphics**]: Three-Dimensional Graphics and Realism—*color, shading, shadowing, and texture*; J.2 [**Computer Applications**]: Physical Science and Engineering—*physics*

General Terms: Algorithms, Theory

Additional Key Words and Phrases: Aberration of light, Doppler effect, Lorentz transformation, shading, shadow, special relativity.

---

## 1. INTRODUCTION

In traditional computer graphics, an underlying assumption is that the speed of light is infinite or the speeds of the scenes relative to the viewer are very small compared to that of light so that the propagation delay of light signals and other relativistic effects can be neglected. For example, in some science-fiction movies and computer games, an object (e.g., a space ship) may move with a speed comparable to that of light, but nothing in its shape, brightness, color, or shadow shows the consequences of special relativity. Although we can not experience directly the fundamental phenomena that special relativity predicts, one would like to experience the

---

Authors' address: National Taiwan University, Department of Computer Science and Information Engineering, Tapei, Taiwan, R.O.C.

Permission to make digital/hard copy of part or all of this work for personal or classroom use is granted without fee provided that the copies are not made or distributed for profit or commercial advantage, the copyright notice, the title of the publication, and its date appear, and notice is given that copying is by permission of the ACM, Inc. To copy otherwise, to republish, to post on servers, or to redistribute to lists, requires prior specific permission and/or a fee.

© 1996 ACM 0730-0301/96/0100-0265 \$03.50

phenomena through science-fiction movies, computer games, or virtual environments. In addition to the main applications for entertainment, the creation of realistic pictures with relativistic effects will also be helpful in learning the concepts of relativity itself, because people usually learn more easily when presented with pictures illustrating the concepts they are learning.

According to special relativity, a moving object with speed  $v$  will be *measured* as contracted in the direction of motion by a factor  $[1 - (v/c)^2]^{1/2}$  (where  $c$  is the speed of light in a vacuum). This phenomenon is called the Lorentz contraction. Ever since Einstein presented his special theory of relativity in 1905 there has been a general belief that the Lorentz contraction could in general be seen or photographed at sufficiently high speeds. For example, Lorentz stated in 1922 that the contraction could be photographed [Terrell 1959]. However, the process of *observing* is different from the process of *seeing*. An observation of the shape of a moving object involves simultaneous measurement of a number of points on the object. If the measurements are optical, then the photons must leave the two points of the object at the same time, as measured by the observer. On the other hand, in seeing or photographing a moving object, it is necessary that photons from various parts of the object arrive at the eye or camera simultaneously. Since the various points of the object are generally at different distances from the eye, the simultaneously arriving photons could not all have left the object simultaneously for the viewer. This distinction was not noticed until 1959, when it was first pointed out by James Terrell [1959]. Terrell showed that a rapidly moving object which subtends a small solid angle with respect to the viewer will appear to have undergone rotation, not contraction. Since Terrell's work, there have been many other papers dedicated to the visual appearance of rapidly moving objects. Weisskopf considered the appearance of moving objects under nonrelativistic conditions (where light moves with light velocity  $c$  only in the stationary frame of reference of the viewer and a moving object is assumed not to suffer a Lorentz contraction) and showed why a rapidly moving object appears to have undergone rotation under relativistic conditions [Weisskopf 1960]. Boas considered the results of removing the restriction that the moving object subtends a small solid angle with respect to the viewer, and showed that spheres always present a circular outline to all viewers and that straight lines may appear curved [Boas 1961]. Scott and Viner showed that the Lorentz contraction is still visible under suitable conditions [Scott and Viner 1965], contrary to an impression which might be taken from some papers on the subject (e.g., see [Terrell 1959]). Scott and Viner also discussed the calculated geometrical appearance of objects moving at relativistic speeds.

In this article, we shall deal with the problem of shading objects which are in relativistic motion. There are no constraints on relative motions between the scene objects, the light sources and the viewer. In addition to

addressing the problem of determining the visual appearance of objects, we shall also treat the following problems: (1) how to determine the scene radiance of a rapidly moving object, (2) how to determine incident irradiance at a scene point coming from a moving light source, (3) how to determine the color of a rapidly moving object, and (4) how to generate shadows for moving objects and moving light sources.

In the next section, some background knowledge of relativity theory, including the Lorentz transformation, the velocity transformation, the aberration of light, and the Doppler effect is reviewed. In Section 3 we shall deal with the problem of determining the apparent appearance of an object moving at relativistic speeds. This section is based on the work performed by Scott and Viner [1965], and it may be regarded as an extension of their work to more general cases. Section 4 treats the problem of determining the apparent scene radiance of a rapidly moving object. In Section 5 we shall deal with the problem of determining the incident irradiance at a scene point coming from a moving light source. Shadow generation is also considered in this section. In Section 6 the shading process for scenes in relativistic motion is summarized and examples are given to demonstrate the effects of shading. In Section 7, a detailed comparison to the work by Hsiung et al. [1990] is presented. We shall describe the difference in methodology and intended goal of the two methods.

## 2. BACKGROUND: SURVEY OF SOME IMPORTANT RESULTS IN RELATIVITY THEORY

### 2.1 Lorentz Transformation

In a given inertial system  $I$ , an event which occurs at a point  $P$  at the time  $t$  can be characterized by four figures, namely, the three coordinates specifying the point  $P$  and the time parameter  $t$ . If, for instance, we use a Cartesian system of coordinates  $S$  in the inertial system  $I$ , the space-time coordinates of the event are  $(x, y, z, t)$ , where  $x, y, z$  are the Cartesian coordinates of the point  $P$ . If we consider another inertial system,  $I'$ , an event in the system will also be specified by four space-time coordinates  $(x', y', z', t')$  defining a space-time system of coordinates  $S'$ . For convenience we shall assume that the Cartesian axes in  $S$  and  $S'$  are parallel to each other and  $S'$  is moving relative to  $S$  with velocity  $\mathbf{v} = (v_x, v_y, v_z)$ . Moreover, let us assume that the origin  $O'$  of  $S'$  coincides with the origin  $O$  of  $S$  at the time  $t = t' = 0$ . Then, the connection between the space-time coordinates  $(x, y, z, t)$  and  $(x', y', z', t')$  of the same event in  $S$  and  $S'$  can be established by the *Lorentz Transformation* (see, e.g., [Møller 1955]).

$$\begin{pmatrix} x \\ y \\ z \\ t \end{pmatrix} = \begin{pmatrix} L_{11}(\mathbf{v}) & L_{12}(\mathbf{v}) & L_{13}(\mathbf{v}) & L_{14}(\mathbf{v}) \\ L_{21}(\mathbf{v}) & L_{22}(\mathbf{v}) & L_{23}(\mathbf{v}) & L_{24}(\mathbf{v}) \\ L_{31}(\mathbf{v}) & L_{32}(\mathbf{v}) & L_{33}(\mathbf{v}) & L_{34}(\mathbf{v}) \\ L_{41}(\mathbf{v}) & L_{42}(\mathbf{v}) & L_{43}(\mathbf{v}) & L_{44}(\mathbf{v}) \end{pmatrix} \begin{pmatrix} x' \\ y' \\ z' \\ t' \end{pmatrix}, \quad (1)$$

where

$$\begin{aligned}
L_{11}(\mathbf{v}) &= 1 + (\gamma - 1)u_x^2/v^2, & L_{12}(\mathbf{v}) &= (\gamma - 1)v_x v_y/v^2, & L_{13}(\mathbf{v}) &= (\gamma - 1)v_x v_z/v^2, \\
L_{14}(\mathbf{v}) &= v_x \gamma, & L_{21}(\mathbf{v}) &= (\gamma - 1)v_y v_x/v^2, & L_{22}(\mathbf{v}) &= 1 + (\gamma - 1)v_y^2/v^2, \\
L_{23}(\mathbf{v}) &= (\gamma - 1)v_y v_z/v^2, & L_{24}(\mathbf{v}) &= v_x \gamma, & L_{31}(\mathbf{v}) &= (\gamma - 1)v_z v_x/v^2, \\
L_{32}(\mathbf{v}) &= (\gamma - 1)v_z v_y/v^2, & L_{33}(\mathbf{v}) &= 1 + (\gamma - 1)v_z^2/v^2, & L_{34}(\mathbf{v}) &= v_z \gamma, \\
L_{41}(\mathbf{v}) &= \gamma v_x/c^2, & L_{42}(\mathbf{v}) &= \gamma v_y/c^2, & L_{43}(\mathbf{v}) &= \gamma v_z/c^2, \\
L_{44}(\mathbf{v}) &= \gamma, & \gamma &= 1/\sqrt{1 - (v/c)^2}, & v &= \|\mathbf{v}\| = \sqrt{v_x^2 + v_y^2 + v_z^2},
\end{aligned}$$

and the constant  $c$  denotes the speed of light in a vacuum. The inverse relations, which can be obtained by solving Eq. (1) with respect to the variables  $x'$ ,  $y'$ ,  $z'$ ,  $t'$ , are

$$\begin{pmatrix} x' \\ y' \\ z' \\ t' \end{pmatrix} = \begin{pmatrix} L_{11}(-\mathbf{v}) & L_{12}(-\mathbf{v}) & L_{13}(-\mathbf{v}) & L_{14}(-\mathbf{v}) \\ L_{21}(-\mathbf{v}) & L_{22}(-\mathbf{v}) & L_{23}(-\mathbf{v}) & L_{24}(-\mathbf{v}) \\ L_{31}(-\mathbf{v}) & L_{32}(-\mathbf{v}) & L_{33}(-\mathbf{v}) & L_{34}(-\mathbf{v}) \\ L_{41}(-\mathbf{v}) & L_{42}(-\mathbf{v}) & L_{43}(-\mathbf{v}) & L_{44}(-\mathbf{v}) \end{pmatrix} \begin{pmatrix} x \\ y \\ z \\ t \end{pmatrix}. \quad (2)$$

## 2.2 Velocity Transformation

It often happens that the velocity of an object is known in one frame of reference, which in turn is moving with respect to a second frame of reference, and we wish to find the velocity of the object in this second frame of reference. Let us again consider the two systems of inertia  $S$  and  $S'$  whose space-time coordinates are connected by Eqs. (1) and (2). The motion of an arbitrarily moving object will then in  $S$  be described by a set of equations:

$$x = x(t), \quad y = y(t), \quad z = z(t). \quad (3)$$

In  $S'$  the same motion is described by the equations

$$x' = x'(t'), \quad y' = y'(t'), \quad z' = z'(t'), \quad (4)$$

which may be obtained from Eq. (3) by means of the Lorentz transformation in Eq. (2).

The velocities of the object relative to  $S$  and  $S'$  are defined, respectively, by:

$$\mathbf{u} = (u_x, u_y, u_z) = \left( \frac{dx}{dt}, \frac{dy}{dt}, \frac{dz}{dt} \right),$$

and

$$\mathbf{u}' = (u'_x, u'_y, u'_z) = \left( \frac{dx'}{dt'}, \frac{dy'}{dt'}, \frac{dz'}{dt'} \right).$$

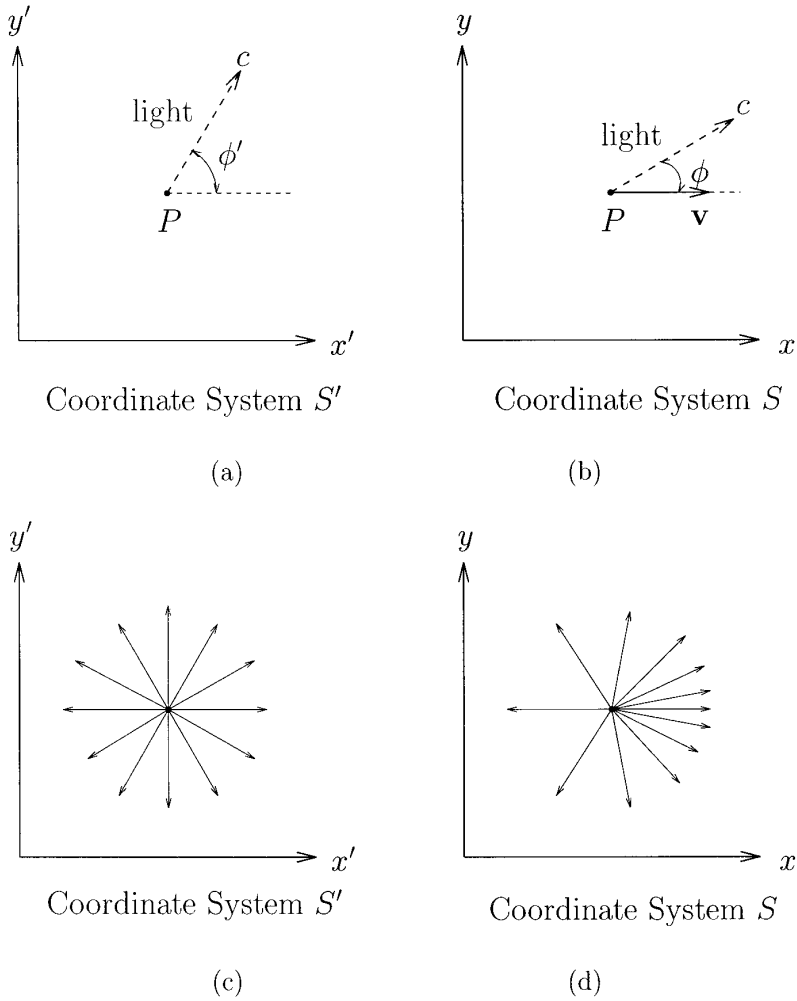


Fig. 1. Aberration of light. (a), (b): A particle  $P$  emits a light beam at an angle  $\phi$  to the  $x'$ -axis in its own coordinate system  $S'$ , however, the light beam makes a new angle  $\phi$  with the  $x$ -axis when viewed in the laboratory coordinate system  $S$ . (c), (d): If the particle emits light uniformly in all directions in  $S'$ , the light is thrown predominantly in the forward direction when viewed in  $S$ .

The equations that relate velocities  $u$  and  $u'$  measured in two different frames of reference are often referred to as the *relativistic velocity addition equations*, which are

$$\mathbf{u} = \frac{\sqrt{1 - (v/c)^2} \mathbf{u}' + \{[1 - \sqrt{1 - (v/c)^2}] (\mathbf{v} \cdot \mathbf{u}'/v^2) + 1\} \mathbf{v}}{1 + (\mathbf{v} \cdot \mathbf{u}'/c^2)},$$

$$\mathbf{u}' = \frac{\sqrt{1 - (v/c)^2} \mathbf{u} + \{[1 + \sqrt{1 - (v/c)^2}] (\mathbf{v} \cdot \mathbf{u}/v^2) - 1\} \mathbf{v}}{1 - (\mathbf{v} \cdot \mathbf{u}/c^2)}.$$

### 2.3 Aberration of Light

If a particle  $P$ , moving through the laboratory coordinate system  $S$  at a speed  $v$  along the  $x$ -axis, emits a light beam at an angle  $\phi'$  to the  $x'$ -axis, as measured in its own coordinate system  $S'$ , the light beam is pushed forward in the laboratory coordinate system  $S$  to a new angle  $\phi$  (as before, we have assumed the axes in  $S$  and  $S'$  coincided at  $t = t' = 0$ ). Figure 1(a) shows the particle  $P$  at rest in its own coordinate system  $S'$  emitting light at an angle  $\phi'$ , and Figure 1(b) shows it moving through the laboratory coordinate system  $S$  where the new angle of emission is  $\phi$ . The relation between  $\phi'$  and  $\phi$  is given by

$$\tan \phi = \frac{\sin \phi' \sqrt{1 - \beta^2}}{\cos \phi' + \beta}, \quad (5)$$

$$\tan \phi' = \frac{\sin \phi \sqrt{1 - \beta^2}}{\cos \phi - \beta},$$

where  $\beta = v/c$ . The phenomenon that the direction of a light beam depends on the velocity of the light source relative to the observer is called *aberration*. Now suppose the particle  $P$  emits light uniformly in all directions, as shown in Figure 1(c). Then, when viewed from the laboratory coordinate system  $S$ , the light is thrown predominantly in a forward direction because of the effect of aberration, as shown in Figure 1(d).

### 2.4 Doppler Effect

The observer of a wave does not always observe the same frequency as that emitted by the source. If either the source or the observer is moving, a different frequency is observed. This phenomenon of frequency shift due to the relative motion of the observer and the source is called the Doppler effect. The Doppler effect for light is described as follows. Let  $P_l$  be a light source moving with respect to the observer with constant velocity  $\mathbf{v}$ , and let the light beam emitted from  $P_l$  have a frequency of  $f'$  as measured in the rest coordinate system of  $P_l$  ( $f'$  is called the proper frequency). If from the viewpoint of the observer, the light beam arrives along the direction of  $\mathbf{V}$ , then the apparent frequency of the light beam for the observer, denoted as  $f$ , is given by

$$f = f' \frac{\sqrt{1 - \beta^2}}{1 - \beta(\mathbf{v} \cdot \mathbf{V} / |\mathbf{v}| |\mathbf{V}|)}, \quad (6)$$

where  $\beta = v/c$ . Notice that when the observer and the light source are approaching each other, the received apparent frequency is greater than the emitted proper frequency, and when they are receding from each other, the received apparent frequency is less than the emitted proper frequency.

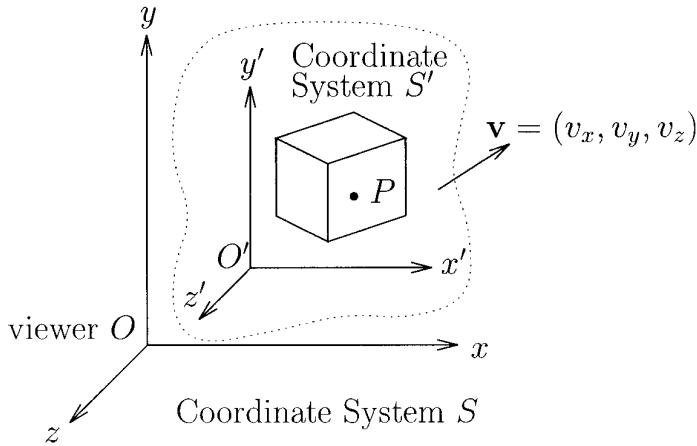


Fig. 2. Coordinate systems used in this paper. The viewer is still at the origin of the coordinate system  $S$ , and the object is at rest in the coordinate system  $S'$ , which is moving relative to  $S$  with a velocity  $\mathbf{v} = (v_x, v_y, v_z)$ .

### 3. APPARENT SHAPE OF RAPIDLY MOVING OBJECTS

When a viewer sees or photographs an object, he records light photons emitted by the object when they arrive simultaneously at the retina or at the photographic film. Since the various points of the object are generally at different distances from the eye (or camera), the simultaneously arriving photons could not all have left the object simultaneously for the viewer. The points further away from the viewer have emitted their part of the picture earlier than have the closer points. Hence, if the object is in motion, the eye or the photograph gets a distorted picture of the object, since the object has been at different locations when different parts of it have emitted the light seen in the picture.

As shown in Figure 2, in the following we shall use  $S$  to denote the coordinate system in which the viewer  $O$  is at rest, and  $S'$  is the rest system of the object. Let  $\mathbf{v} = (v_x, v_y, v_z)$  be the velocity of  $S'$  relative to  $S$ , and let the axes of  $S$  and  $S'$  be parallel to each other and the two origins  $O$  and  $O'$  coincide at  $t = t' = 0$ . Then the Lorentz transformation formulae connecting  $S$  and  $S'$  are just like those given in Eqs. (1) and (2). Since an event might have different space-time coordinates with respect to different coordinate systems, when it is necessary we shall add a subscript, such as  $S$  or  $S'$ , to the space-time coordinates of an event to emphasize the coordinate system in which the space-time coordinates are specified.

Since an object in any shape can be approximated by a net of planar polygonal facets, let us first consider the visual appearance of a plane in motion. Suppose the plane passes through a point  $(x'_0, y'_0, z'_0)_{S'}$  in its own rest coordinate system  $S'$  and has a plane normal  $(A, B, C)_{S'}$ ; then it can be represented in  $S'$  by the equation

$$A(x' - x'_0) + B(y' - y'_0) + C(z' - z'_0) = 0. \quad (7)$$

Consider a point  $P$  on the plane with space coordinates  $(x', y', z')_{S'}$ , and we want to determine the *apparent position* of point  $P$  with respect to the viewer  $O$  who sees or photographs the plane at the instant  $t = t_s$  (where  $t$  is the time parameter of  $S$ ;  $t_s$  is a constant and we shall call it the seeing time in the following). We call  $(x, y, z)_S$  the apparent position of point  $P$  if, at the instant  $t = [t_s - (x^2 + y^2 + z^2)^{1/2}/c]$ ,  $P$  is at  $(x, y, z)_S$  such that the light emitted from point  $P(x, y, z)_S$  at that instant will arrive at the viewer  $O$  exactly at the instant  $t = t_s$  (the propagation delay of light signals from  $(x, y, z)_S$  to  $(0, 0, 0)$  accounts for the term  $\frac{1}{c}(x^2 + y^2 + z^2)^{1/2}$ ). Figure 3 illustrates the idea more clearly. In this figure, **Event 1** represents the place and time that  $P$  emits the photons that will arrive at the viewer  $O$  at  $t = t_s$ , and **Event 2** represents the place and time that the viewer  $O$  receives the photons. From the viewpoint of coordinate system  $S$ , the light is emitted from  $P(x, y, z)_S$  to  $(0, 0, 0)_S$  and the transmission of light signals takes  $\frac{1}{c}(x^2 + y^2 + z^2)^{1/2}$  units of time. However, from the viewpoint of coordinate system  $S'$ , the light is emitted from  $P(x', y', z')_{S'}$  to  $(-v_x \gamma t_s - v_y \gamma t_s, -v_z \gamma t_s)_{S'}$ , and the transmission of light signals takes  $[\gamma/c^2(v_x x + v_y y + v_z z) + \gamma/c(x^2 + y^2 + z^2)^{1/2}]$  units of time. From the Lorentz transformation given in Eq. (2),  $x', y', z', t'$ , can be expressed in terms of  $x, y, z$ :

$$\begin{aligned} x' &= L_{11}(-\mathbf{v})x + L_{12}(-\mathbf{v})y + L_{13}(-\mathbf{v})z + L_{14}(-\mathbf{v}) \cdot [t_s - (x^2 + y^2 + z^2)^{1/2}/c], \\ y' &= L_{21}(-\mathbf{v})x + L_{22}(-\mathbf{v})y + L_{23}(-\mathbf{v})z + L_{24}(-\mathbf{v}) \cdot [t_s - (x^2 + y^2 + z^2)^{1/2}/c], \\ z' &= L_{31}(-\mathbf{v})x + L_{32}(-\mathbf{v})y + L_{33}(-\mathbf{v})z + L_{34}(-\mathbf{v}) \cdot [t_s - (x^2 + y^2 + z^2)^{1/2}/c], \\ t' &= L_{41}(-\mathbf{v})x + L_{42}(-\mathbf{v})y + L_{43}(-\mathbf{v})z + L_{44}(-\mathbf{v}) \cdot [t_s - (x^2 + y^2 + z^2)^{1/2}/c]. \end{aligned} \quad (8)$$

Since  $P(x', y', z')_{S'}$  is on the plane specified by Eq. (7),  $(x', y', z')$  must satisfy Eq. (7). Substituting Eq. (8) into Eq. (7) gives

$$\begin{aligned} & [A \cdot L_{11}(-\mathbf{v}) + B \cdot L_{21}(-\mathbf{v}) + C \cdot L_{31}(-\mathbf{v})]x \\ & + [A \cdot L_{12}(-\mathbf{v}) + B \cdot L_{22}(-\mathbf{v}) + C \cdot L_{32}(-\mathbf{v})]y \\ & + [A \cdot L_{13}(-\mathbf{v}) + B \cdot L_{23}(-\mathbf{v}) + C \cdot L_{33}(-\mathbf{v})]z \\ & + [A \cdot L_{14}(-\mathbf{v}) + B \cdot L_{24}(-\mathbf{v}) + C \cdot L_{34}(-\mathbf{v})] \cdot [t_s - (x^2 + y^2 + z^2)^{1/2}/c] \\ & - (Ax'_0 + By'_0 + Cz'_0) = 0, \end{aligned} \quad (9)$$

which represents the visual appearance of the plane under consideration with respect to the viewer  $O$  with the seeing time  $t_s$ .

In general, if the original shape of an object, as described in its own rest

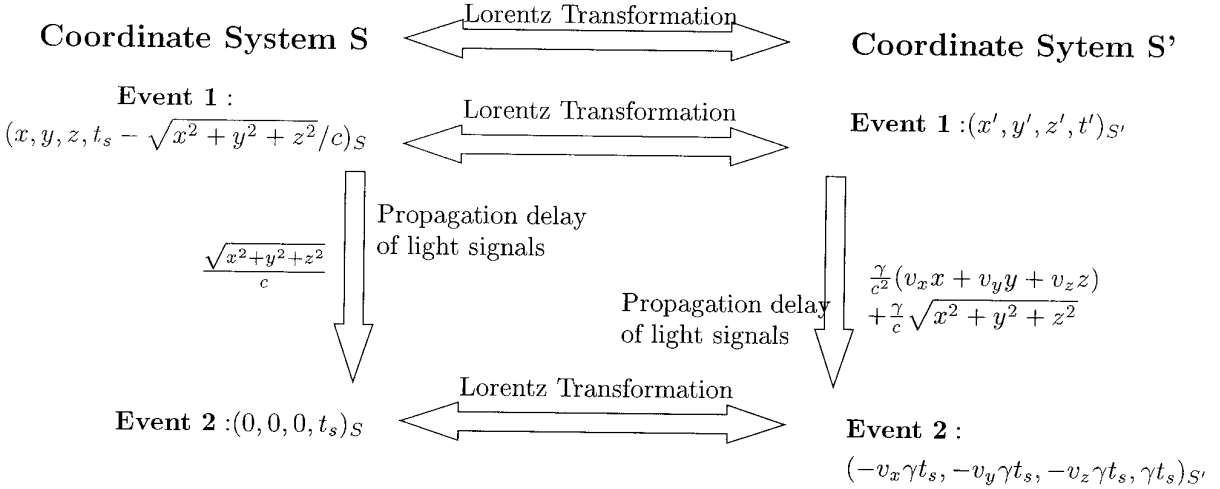


Fig. 3. The relations between the space-time coordinates of **Event 1** and **Event 2**.

coordinate system  $S'$ , is given by the system of equations

$$\begin{aligned}
 f'_1(x', y', z') &= 0, \\
 f'_2(x', y', z') &= 0, \\
 &\vdots \\
 f'_n(x', y', z') &= 0,
 \end{aligned}
 \tag{10}$$

then we can obtain the apparent shape of the object with respect to the viewer  $O$  with seeing time  $t_s$  by expressing the  $(x', y', z')$  in Eq. (10) in terms of  $(x, y, z)$  (i.e., substituting Eq. (8) into Eq. (10)):

$$\begin{aligned}
 f_1(x, y, z) &= f'_1(x'(x, y, z), y'(x, y, z), z'(x, y, z)) = 0, \\
 f_2(x, y, z) &= f'_2(x'(x, y, z), y'(x, y, z), z'(x, y, z)) = 0, \\
 &\vdots \\
 f_n(x, y, z) &= f'_n(x'(x, y, z), y'(x, y, z), z'(x, y, z)) = 0.
 \end{aligned}
 \tag{11}$$

#### 4. SCENE RADIANCE OF RAPIDLY MOVING OBJECTS

In the last section, we dealt with the problem of where some point on the rapidly moving object will appear on the image. In the next two sections we shall deal with the problem of how bright the image of some surface on the rapidly moving object will be. The image intensity is proportional to the scene radiance (the power per unit of foreshortened area emitted into a unit

solid angle), and the scene radiance depends on (1) the amount of light that falls on the surface, (2) the fraction of the incident light that is reflected, and (3) the direction from which the surface is viewed and from which it is illuminated. Mathematically, we can use the *bidirectional reflectance distribution function*  $BRDF(\theta_r, \phi_r, \theta_i, \phi_i)$  to describe the characteristics of a surface. The  $BRDF(\theta_r, \phi_r, \theta_i, \phi_i)$  specifies how bright a surface appears when viewed from one direction while light falls on it from another. The direction of incident and reflected light rays can be specified in a local coordinate system by using polar angle  $\theta$  and azimuth angle  $\phi$ . Let the amount of light falling on the surface from the direction  $(\theta'_i, \phi'_i)$ —the irradiance—be  $J^{i'}(\theta'_i, \phi'_i)$ , and let the brightness of the surface as seen from the direction  $(\theta'_r, \phi'_r)$ —the radiance—be  $J^{r'}(\theta'_r, \phi'_r)$ . Then the differential reflectance model can be described as

$$dJ^{r'}(\theta'_r, \phi'_r, \theta'_i, \phi'_i) = dJ^{i'}(\theta'_i, \phi'_i) \cdot BRDF(\theta'_i, \phi'_i, \theta'_r, \phi'_r). \quad (12)$$

This equation states that the differential emitted radiance ( $\text{w/m}^2\text{-sr}$ ) in the direction  $(\theta'_r, \phi'_r)$  is equal to the incident differential irradiance  $dJ^{i'}(\theta'_i, \phi'_i)$  ( $\text{w/m}^2$ ) times the bidirectional reflectance distribution function  $BRDF(\theta'_i, \phi'_i, \theta'_r, \phi'_r)$  ( $1/\text{sr}$ ). To determine the radiance from the differential form, we must integrate the product of the  $BRDF$  and the irradiance over the hemisphere of possible directions from which light can fall on a surface. Thus,

$$J^{r'}(\theta'_r, \phi'_r) = \int_{\theta'_i=0}^{\pi/2} \int_{\phi'_i=0}^{2\pi} dJ^{i'}(\theta'_i, \phi'_i, \theta'_r, \phi'_r) \sin \theta'_i d\theta'_i d\phi'_i. \quad (13)$$

In Eqs. (12) and (13), we have used the superscript prime to emphasize that the equation is described with respect to the coordinate system  $S'$ , in which the object is at rest. Now the problems are (1) if the light sources are not stationary relative to the scenes, how to determine the scene irradiance contributed from the moving light sources, and (2) if the radiance at a scene point in coordinate system  $S'$ ,  $J^{r'}(\theta'_r, \phi'_r)$ , is already known, how to determine the apparent radiance at the scene point,  $J^r(\theta_r, \phi_r)$ , for a viewer at rest in  $S$ .

Since the two problems may be solved separately, for convenience we shall consider the second problem first, and the first problem is left to the next section.

Figures 4 and 5 illustrate why, for the same scene point, the value of  $J^{r'}(\theta'_r, \phi'_r)$  is generally different from that of  $J^r(\theta_r, \phi_r)$ . In Figure 4(a), let us consider a scene point  $P'(x', y', z')_{S'}$  on the plane whose equation w.r.t. the coordinate system  $S'$  is given as in Eq. (7). Let  $J^{r'}(\theta'_r, \phi'_r)$  be the radiance at  $P'(x', y', z')_{S'}$ , and let  $dA'$  be the area of a small planar patch centered at  $P'(x', y', z')_{S'}$ . Then the differential radiant power  $d\phi'$  emitted from the planar patch  $dA'$  through a viewing cone of solid angle

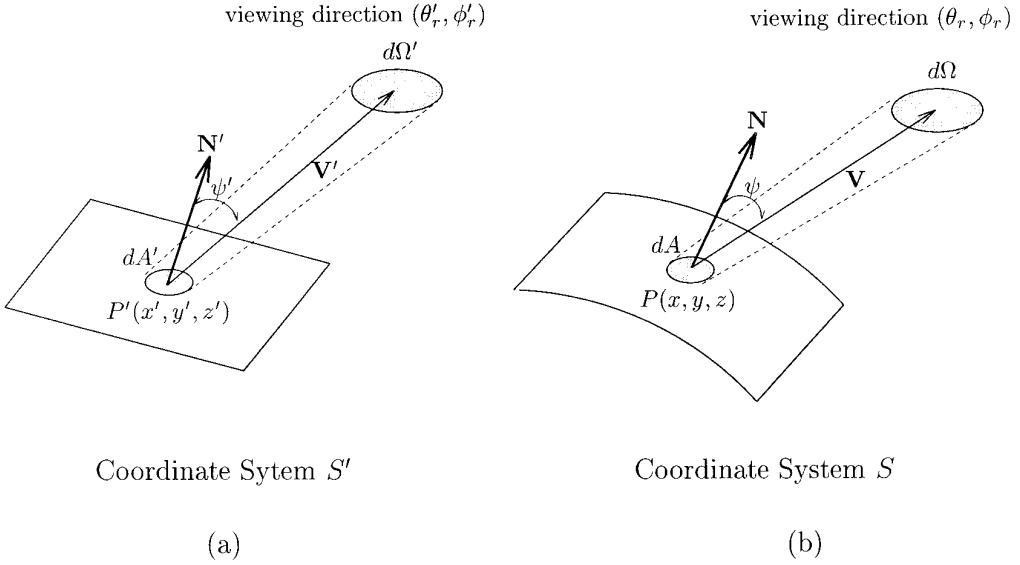


Fig. 4. The scene radiance  $J^r(\theta_r, \phi_r)$  might be different from  $J^{r'}(\theta_r', \phi_r')$  because the values of  $dA'$ ,  $d\Omega'$ ,  $(\theta_r', \phi_r')$  may be different from those of  $dA$ ,  $d\Omega$ ,  $(\theta_r, \phi_r)$ .

$d\varphi'$  in the direction  $(\theta_r', \phi_r')$  is

$$d\varphi' = J^{r'}(\theta_r', \phi_r') \cos \psi' dA' d\Omega', \tag{14}$$

where  $\psi'$  is the angle that the viewing direction  $(\theta_r', \phi_r')$  makes with the plane normal  $\mathbf{N}' = (A, B, C)$ , and the term  $\cos \psi'$  accounts for the foreshortening of the planar patch  $dA'$  as seen from the direction  $(\theta_r', \phi_r')$ . However, from the viewpoint of a viewer at rest in  $S$  (see Figure 4(b)), the same amount of radiant power  $d\varphi'$  is emitted from a surface patch of area  $dA$  flowing into a viewing cone of solid angle  $d\Omega$  in the direction  $(\theta_r, \phi_r)$ , where the values  $dA$ ,  $d\Omega$ , and  $(\theta_r, \phi_r)$  might be very different from those of  $dA'$ ,  $d\Omega'$ , and  $(\theta_r', \phi_r')$ . Figure 5 illustrates why they are different. For convenience, let us assume the small planar patch  $dA'$  in Figure 4(a) is discretely composed of radiating particles  $P'_1, P'_2, \dots, P'_6$ , as shown in Figure 5(a). The particles  $P'_1, P'_2, \dots, P'_6$  are assumed to be spaced evenly and emit light uniformly in all directions. According to the discussion of the last section, the apparent positions of  $P'_1, P'_2, \dots, P'_6$  w.r.t. a viewer at rest in  $S$ , denoted as  $P_1, P_2, \dots, P_6$  in Figure 5(b), might no longer be spaced evenly, so the area of surface patch  $dA$  comprising  $P_1, P_2, \dots, P_6$  might be different from that of  $dA'$ . Moreover, because of aberration of light, the light emitted from each of  $P_1, P_2, \dots, P_6$  is no longer distributed uniformly in all directions, and the angle that the viewing direction makes with the surface normal might vary. Hence, to find the relation between  $J^r(\theta_r, \phi_r)$  and  $J^{r'}(\theta_r', \phi_r')$ , we must first find the relations between  $\cos \psi$  and  $\cos \psi'$ ,  $dA$  and  $dA'$ ,  $d\Omega$  and  $d\Omega'$ .

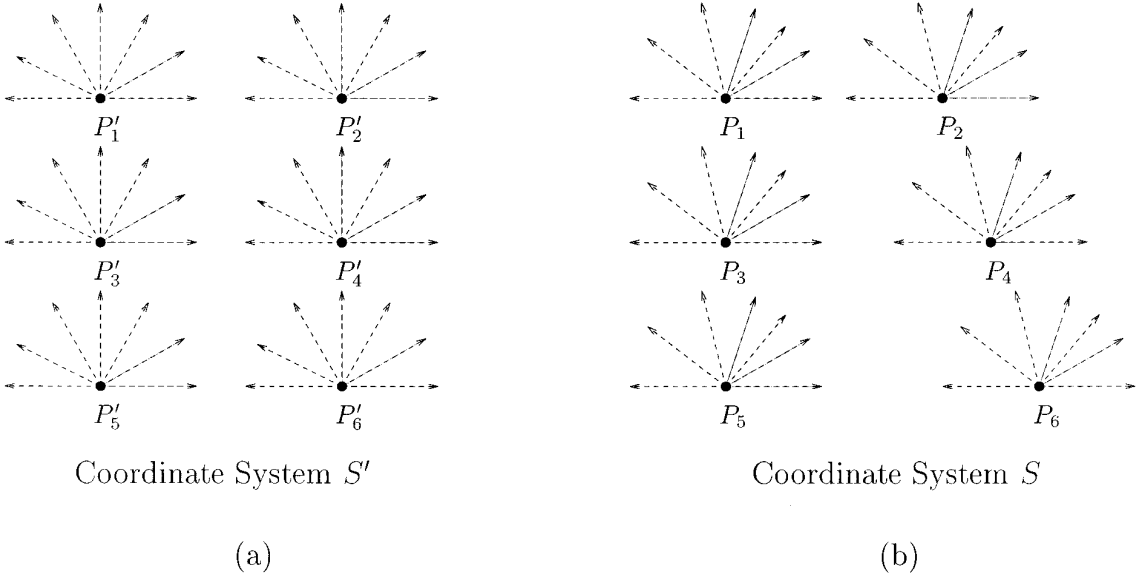


Fig. 5. (a) In the rest system of the object  $S'$ , the radiating particles  $P'_1, P'_2, \dots, P'_6$  are spaced evenly and emit light uniformly in all directions; (b) from the viewpoint of a viewer at rest in the coordinate system  $S$ , those particles are no longer spaced evenly and the light emitted from them is not distributed uniformly in all directions.

#### 4.1 Relation between $\cos \psi$ and $\cos \psi'$

According to the discussion of the previous section, the differential surface patch  $dA$  is located on the surface specified by Eq. (9), which can be rewritten as

$$F(x, y, z) = \kappa_1 x + \kappa_2 y + \kappa_3 z + \kappa_4 [t_s - (x^2 + y^2 + z^2)^{1/2}/c] + \kappa_5 = 0, \quad (15)$$

where

$$\begin{aligned} \kappa_1 &= A \cdot L_{11}(-\mathbf{v}) + B \cdot L_{21}(-\mathbf{v}) + C \cdot L_{31}(-\mathbf{v}), \\ \kappa_2 &= A \cdot L_{12}(-\mathbf{v}) + B \cdot L_{22}(-\mathbf{v}) + C \cdot L_{32}(-\mathbf{v}), \\ \kappa_3 &= A \cdot L_{13}(-\mathbf{v}) + B \cdot L_{23}(-\mathbf{v}) + C \cdot L_{33}(-\mathbf{v}), \\ \kappa_4 &= A \cdot L_{14}(-\mathbf{v}) + B \cdot L_{24}(-\mathbf{v}) + C \cdot L_{34}(-\mathbf{v}), \\ \kappa_5 &= -(Ax'_0 + By'_0 + Cz'_0). \end{aligned} \quad (16)$$

The surface normal at  $P(x, y, z)_S$  is

$$\mathbf{N} = \frac{1}{\sqrt{F_x^2 + F_y^2 + F_z^2}} (F_x, F_y, F_z), \quad (17)$$

where

$$\begin{aligned}
 F_x &= \frac{\partial F}{\partial x} = \kappa_1 - \frac{\kappa_4 x}{c\sqrt{x^2 + y^2 + z^2}}, \\
 F_y &= \frac{\partial F}{\partial y} = \kappa_2 - \frac{\kappa_4 y}{c\sqrt{x^2 + y^2 + z^2}}, \\
 F_z &= \frac{\partial F}{\partial z} = \kappa_3 - \frac{\kappa_4 z}{c\sqrt{x^2 + y^2 + z^2}}.
 \end{aligned} \tag{18}$$

From the viewpoint of the viewer  $O$  at the origin of system  $S$ , the light is emitted from  $P(x, y, z)_S$  to  $O(0, 0, 0)_S$ . Thus, the viewing direction vector  $\mathbf{V}$  in Figure 4(b) is

$$\mathbf{V} = \frac{-1}{\sqrt{x^2 + y^2 + z^2}} (x, y, z). \tag{19}$$

Now,  $\cos \psi$  can be obtained by taking the inner product of  $\mathbf{N}$  and  $\mathbf{V}$ :

$$\begin{aligned}
 \cos \psi &= \mathbf{N} \cdot \mathbf{V} \\
 &= \frac{-\kappa_1 x - \kappa_2 y - \kappa_3 z + \kappa_4 (x^2 + y^2 + z^2)^{1/2}/c}{\sqrt{x^2 + y^2 + z^2} \sqrt{F_x^2 + F_y^2 + F_z^2}}.
 \end{aligned}$$

Substituting Eq. (15) into the above equation leads to

$$\cos \psi = \frac{\kappa_4 t_s + \kappa_5}{\sqrt{x^2 + y^2 + z^2} \sqrt{F_x^2 + F_y^2 + F_z^2}}. \tag{20}$$

On the other hand, the plane normal at  $P'(x', y', z')_{S'}$  is given by

$$\mathbf{N}' = \frac{1}{\sqrt{A^2 + B^2 + C^2}} (A, B, C). \tag{21}$$

From the viewpoint of the object rest system  $S'$ , the light is emitted from  $P'(x', y', z')_{S'}$ , to  $(-v_x \gamma t_s, -v_y \gamma t_s, -v_z \gamma t_s)_{S'}$  (see Figure 3). Thus, the viewing direction vector  $\mathbf{V}'$  is given by

$$\begin{aligned}
 \mathbf{V}' &= \frac{-(v_x \gamma t_s + x', \quad v_y \gamma t_s + y', \quad v_z \gamma t_s + z')}{\sqrt{(v_x \gamma t_s + x')^2 + (v_y \gamma t_s + y')^2 + (v_z \gamma t_s + z')^2}} \\
 &= \frac{-1}{c|\gamma t_s - t'|} (v_x \gamma t_s + x', \quad v_y \gamma t_s + y', \quad v_z \gamma t_s + z').
 \end{aligned} \tag{22}$$

Now  $\cos \psi'$  can be obtained by taking the inner product of  $\mathbf{N}'$  and  $\mathbf{V}'$ :

$$\begin{aligned} \cos \psi' &= \mathbf{N}' \cdot \mathbf{V}' \\ &= \frac{-Av_x \gamma t_s - Bv_y \gamma t_s - Cv_z \gamma t_s - Ax' - By' - Cz'}{c|\gamma t_s - t'| \sqrt{A^2 + B^2 + C^2}}. \end{aligned}$$

From Eqs. (7) and (16), the above equation can be rewritten as

$$\cos \psi' = \frac{\kappa_4 t_s + \kappa_5}{c|\gamma t_s - t'| \sqrt{A^2 + B^2 + C^2}}. \quad (23)$$

Thus, from Eqs. (20) and (23), we get the relation between  $\cos \psi$  and  $\cos \psi'$ :

$$\cos \psi' = \frac{\sqrt{x^2 + y^2 + z^2} \sqrt{F_x^2 + F_y^2 + F_z^2}}{c|\gamma t_s - t'| \sqrt{A^2 + B^2 + C^2}} \cos \psi. \quad (24)$$

#### 4.2 Relation between $dA$ and $dA'$

The differential area  $dA'$  can be expressed in terms of  $dx'dy'$ :

$$dA' = \frac{\sqrt{A^2 + B^2 + C^2}}{|C|} dx'dy'.$$

Similarly, the differential area  $dA$  can be expressed in terms of  $dxdy$ :

$$dA = \frac{\sqrt{F_x^2 + F_y^2 + F_z^2}}{|F_z|} dxdy,$$

where  $F_x, F_y, F_z$  are given in Eq. (18).  $dx'dy'$  and  $dxdy$  are related by the Jacobian of  $x'$  and  $y'$  with respect to  $x$  and  $y$ , denoted by  $\partial(x', y')/\partial(x, y)$ . The relation is given by

$$dx'dy' = \left| \frac{\partial(x', y')}{\partial(x, y)} \right| dxdy, \quad (25)$$

where  $\partial(x', y')/\partial(x, y)$  is defined as

$$\frac{\partial(x', y')}{\partial(x, y)} = \begin{vmatrix} \frac{\partial x'}{\partial x} & \frac{\partial x'}{\partial y} \\ \frac{\partial y'}{\partial x} & \frac{\partial y'}{\partial y} \end{vmatrix} = \frac{\partial x'}{\partial x} \frac{\partial y'}{\partial y} - \frac{\partial y'}{\partial x} \frac{\partial x'}{\partial y}. \quad (26)$$

From Eq. (8), we have

$$\begin{aligned}
\frac{\partial x'}{\partial x} &= L_{11}(-\mathbf{v}) + L_{13}(-\mathbf{v}) \frac{\partial z}{\partial x} + L_{14}(-\mathbf{v}) \left[ \frac{1}{c\sqrt{x^2 + y^2 + z^2}} \left( x + z \frac{\partial z}{\partial x} \right) \right], \\
\frac{\partial y'}{\partial y} &= L_{22}(-\mathbf{v}) + L_{23}(-\mathbf{v}) \frac{\partial z}{\partial y} + L_{24}(-\mathbf{v}) \left[ \frac{1}{c\sqrt{x^2 + y^2 + z^2}} \left( y + z \frac{\partial z}{\partial y} \right) \right], \\
\frac{\partial x'}{\partial y} &= L_{12}(-\mathbf{v}) + L_{13}(-\mathbf{v}) \frac{\partial z}{\partial y} + L_{14}(-\mathbf{v}) \left[ \frac{1}{c\sqrt{x^2 + y^2 + z^2}} \left( y + z \frac{\partial z}{\partial y} \right) \right], \\
\frac{\partial y'}{\partial x} &= L_{21}(-\mathbf{v}) + L_{23}(-\mathbf{v}) \frac{\partial z}{\partial x} + L_{24}(-\mathbf{v}) \left[ \frac{1}{c\sqrt{x^2 + y^2 + z^2}} \left( x + z \frac{\partial z}{\partial x} \right) \right].
\end{aligned} \tag{27}$$

Substituting Eq. (27) into Eq. (26) and simplifying, we obtain

$$\begin{aligned}
\frac{\partial(x', y')}{\partial(x, y)} &= 1 + (\gamma - 1) \frac{v_x^2}{v^2} + (\gamma - 1) \frac{v_y^2}{v^2} + (\gamma - 1) \frac{v_x v_z}{v^2} \frac{\partial z}{\partial x} + (\gamma - 1) \frac{v_y v_z}{v^2} \frac{\partial z}{\partial y} \\
&\quad - \gamma v_x \left[ \frac{1}{c\sqrt{x^2 + y^2 + z^2}} \left( x + z \frac{\partial z}{\partial x} \right) \right] - \gamma v_y \left[ \frac{1}{c\sqrt{x^2 + y^2 + z^2}} \left( y + z \frac{\partial z}{\partial y} \right) \right].
\end{aligned} \tag{28}$$

From Eq. (18), we have

$$\begin{aligned}
\frac{\partial z}{\partial x} &= -\frac{F_x}{F_z} = -\left( \kappa_1 - \frac{\kappa_4 x}{c\sqrt{x^2 + y^2 + z^2}} \right) \Big/ F_z, \\
\frac{\partial z}{\partial y} &= -\frac{F_y}{F_z} = -\left( \kappa_2 - \frac{\kappa_4 y}{c\sqrt{x^2 + y^2 + z^2}} \right) \Big/ F_z.
\end{aligned} \tag{29}$$

Substituting Eq. (29) into Eq. (28) and simplifying lead to

$$\begin{aligned}
\frac{\partial(x', y')}{\partial(x, y)} &= \left[ \frac{c|C|}{\sqrt{x^2 + y^2 + z^2}} \left( \frac{\gamma\sqrt{x^2 + y^2 + z^2}}{c} + \frac{\gamma v_x x}{c^2} + \frac{\gamma v_y y}{c^2} + \frac{\gamma v_z z}{c^2} \right) \right] \Big/ F_z \\
&= \left[ \frac{c|C|}{\sqrt{x^2 + y^2 + z^2}} \right. \\
&\quad \left. \left( \frac{L_{44}(-\mathbf{v})\sqrt{x^2 + y^2 + z^2}}{c} - L_{44}(-\mathbf{v})x - L_{42}(-\mathbf{v})y - L_{43}(-\mathbf{v})z \right) \right] \Big/ F_z \\
&= \left[ \frac{c|C|\gamma t_s - t'}{\sqrt{x^2 + y^2 + z^2}} \right] \Big/ F_z.
\end{aligned}$$

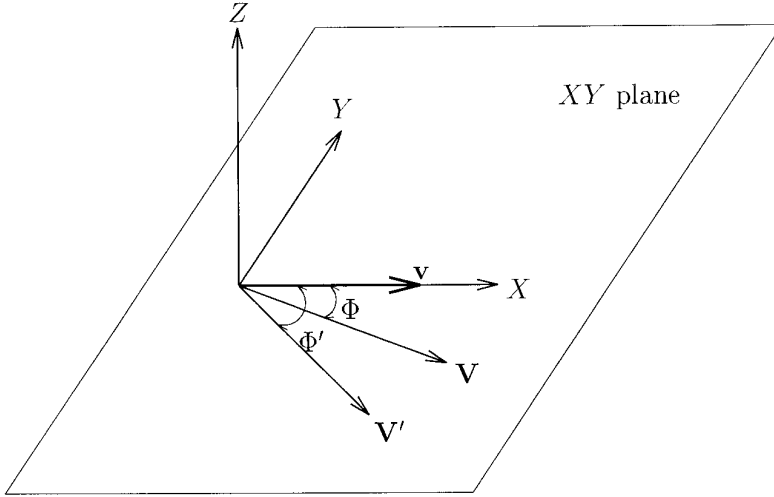


Fig. 6. The XYZ-coordinate system. In this coordinate system, the viewing direction vectors  $\mathbf{V}$  and  $\mathbf{V}'$  fall on the XY-plane.

Consequently, the relation between  $dA$  and  $dA'$  is

$$dA' = \frac{\sqrt{A^2 + B^2 + C^2}}{\sqrt{F_x^2 + F_y^2 + F_z^2}} \frac{c|\gamma t_s - t'|}{\sqrt{x^2 + y^2 + z^2}} dA. \tag{30}$$

### 4.3 Relation between $d\Omega$ and $d\Omega'$

$d\Omega$  and  $d\Omega'$  can be expressed as

$$d\Omega = \sin \theta d\theta d\phi,$$

$$d\Omega' = \sin \theta' d\theta' d\phi'.$$

However, since the polar and azimuth angles are specified in a local coordinate system, we can freely choose a new coordinate system, like the XYZ-coordinate system shown in Figure 6, such that the viewing direction vectors  $\mathbf{V}$  and  $\mathbf{V}'$  fall on the XY-plane. In the XYZ-coordinate system, the direction of  $\mathbf{V}$  can be specified with polar angle  $\Theta = \pi/2$  and azimuth angle  $\Phi$ ; the direction of  $\mathbf{V}'$  can be specified with polar angle  $\Theta' = \pi/2$  and azimuth angle  $\Phi'$ . According to the formula of aberration given in Eq. (5), we have

$$\Theta' = \Theta, \tag{31}$$

$$\tan \Phi' = \frac{\sin \Phi \sqrt{1 - \beta^2}}{\cos \Phi - \beta}.$$

The differential solid angle  $d\Omega$  and  $d\Omega'$  now can be expressed as

$$d\Omega = \sin \Theta d\Theta d\Phi = \sin(\pi/2)d\Theta d\Phi = d\Theta d\Phi,$$

$$d\Omega' = \sin \Theta' d\Theta' d\Phi' = \sin(\pi/2)d\Theta' d\Phi' = d\Theta' d\Phi'.$$

To determine the relation between  $d\Theta d\Phi$  and  $d\Theta' d\Phi'$ , we must first find the Jacobian of  $\Theta$  and  $\Phi$  w.r.t.  $\Theta'$  and  $\Phi'$ ,

$$\frac{\partial(\Theta', \Phi')}{\partial(\Theta, \Phi)} = \begin{vmatrix} \frac{\partial\Theta'}{\partial\Theta} & \frac{\partial\Theta'}{\partial\Phi} \\ \frac{\partial\Phi'}{\partial\Theta} & \frac{\partial\Phi'}{\partial\Phi} \end{vmatrix}.$$

From Eq. (31), we have

$$\frac{\partial\Theta'}{\partial\Theta} = 1, \quad \frac{\partial\Theta'}{\partial\Phi} = 0, \quad \text{and} \quad \frac{\partial\Phi'}{\partial\Theta} = 0.$$

Thus,

$$\frac{\partial(\Theta', \Phi')}{\partial(\Theta, \Phi)} = \frac{\partial\Phi'}{\partial\Phi}.$$

Again, from Eq. (31), we have

$$d(\tan \Phi') = d\left(\frac{\sin \Phi \sqrt{1 - \beta^2}}{\cos \Phi - \beta}\right). \quad (32)$$

Thus,

$$\sec^2\Phi' \cdot d\Phi' = \frac{\sqrt{1 - \beta^2}(1 - \beta \cos \Phi)}{(\cos \Phi - \beta)^2} d\Phi. \quad (33)$$

Since  $\sec^2\Phi' = \tan^2\Phi' + 1$ , we have

$$\sec^2\Phi' = \frac{(1 - \beta \cos \Phi)^2}{(\cos \Phi - \beta)^2}. \quad (34)$$

Substituting Eq. (34) into Eq. (33) yields

$$d\Phi' = \frac{\sqrt{1 - \beta^2}}{1 - \beta \cos \Phi} d\Phi.$$

Hence, we get

$$d\Omega' = d\Theta' d\Phi' = \left| \frac{\partial(\Theta', \Phi')}{\partial(\Theta, \Phi)} \right| d\Theta d\Phi = \frac{\sqrt{1 - \beta^2}}{1 - \beta \cos \Phi} d\Theta d\Phi = \frac{\sqrt{1 - \beta^2}}{1 - \beta \cos \Phi} d\Omega. \quad (35)$$

Since  $\Phi$  is the angle that the object velocity  $\mathbf{v}$  makes with the viewing direction vector  $\mathbf{V}$ ,  $\cos \Phi$  can be expressed as follows:

$$\cos \Phi = \frac{\mathbf{v} \cdot \mathbf{V}}{|\mathbf{v}| |\mathbf{V}|}.$$

Substituting the above equation into Eq. (35) yields

$$d\Omega' = \frac{\sqrt{1 - \beta^2}}{1 - \beta(\mathbf{v} \cdot \mathbf{V}/|\mathbf{v}| |\mathbf{V}|)} d\Omega, \quad (36)$$

which is the relation between  $d\Omega$  and  $d\Omega'$ .

Having found the relations between  $\cos \psi$  and  $\cos \psi'$ ,  $dA$  and  $dA'$ , and  $d\Omega$  and  $d\Omega'$ , now we can determine the apparent scene radiance  $J^r(\mathbf{V}(\theta_r, \phi_r))$ . From the definition of radiance,  $J^r(\mathbf{V}(\theta_r, \phi_r))$  can be expressed as

$$J^r(\mathbf{V}(\theta_r, \phi_r)) = \frac{d\varphi'}{\cos \psi dA d\Omega}.$$

Substituting Eq. (14) into the above equation gives

$$J^r(\mathbf{V}(\theta_r, \phi_r)) = \frac{J^r(\mathbf{V}'(\theta'_r, \phi'_r)) \cos \psi' dA' d\Omega'}{\cos \psi dA d\Omega}. \quad (37)$$

From the relations in Eqs. (24), (30), and (36), we get

$$\begin{aligned} & \frac{\cos \psi' dA' d\Omega'}{\cos \psi dA d\Omega} \\ &= \left( \frac{\sqrt{x^2 + y^2 + z^2} \sqrt{F_x^2 + F_y^2 + F_z^2}}{c|\gamma t_s - t'| \sqrt{A^2 + B^2 + C^2}} \cos \psi \right) \times \left( \frac{\sqrt{A^2 + B^2 + C^2}}{\sqrt{F_x^2 + F_y^2 + F_z^2}} \frac{c|\gamma t_s - t'|}{\sqrt{x^2 + y^2 + z^2}} dA \right) \\ & \times \left( \frac{\sqrt{1 - \beta^2}}{1 - \beta(\mathbf{v} \cdot \mathbf{V}/|\mathbf{v}| |\mathbf{V}|)} d\Omega \right) / (\cos \psi dA d\Omega). \end{aligned}$$

Notice the effect of  $\cos \psi'$  variation (the first term in the above equation) counteracts the effect of  $dA'$  variation (the second term in the above equation) such that the foreshortened area  $\cos \psi' dA'$  seen from direction

$\mathbf{V}'$  in coordinate system  $S'$  equals the foreshortened area  $\cos \psi dA$  seen from direction  $\mathbf{V}$  in coordinate system  $S$ . Thus, we have

$$\frac{\cos \psi' dA' d\Omega'}{\cos \psi dA d\Omega} = \frac{\sqrt{1 - \beta^2}}{1 - \beta(\mathbf{v} \cdot \mathbf{V}/|\mathbf{v}\|\|\mathbf{V}\|)}.$$

Substituting the above equation into Eq. (37), we get the relation between  $J^r(\mathbf{V}(\theta_r, \phi_r))$  and  $J^{r'}(\mathbf{V}'(\theta'_r, \phi'_r))$ :

$$J^r(\mathbf{V}(\theta_r, \phi_r)) = \frac{\sqrt{1 - \beta^2}}{1 - \beta(\mathbf{v} \cdot \mathbf{V}/|\mathbf{v}\|\|\mathbf{V}\|)} J^{r'}(\mathbf{V}'(\theta'_r, \phi'_r)). \quad (38)$$

The above equation has overlooked the Doppler effect. When the Doppler effect is taken into account, the scene radiance can be expressed as a spectral energy distribution function of wavelength and Eq. (38) can be written as

$$J^r(\mathbf{V}(\theta_r, \phi_r), \lambda) = \frac{\sqrt{1 - \beta^2}}{1 - \beta(\mathbf{v} \cdot \mathbf{V}/|\mathbf{v}\|\|\mathbf{V}\|)} J^{r'}(\mathbf{V}'(\theta'_r, \phi'_r), \lambda'), \quad (39)$$

where  $\lambda'$  is the observed wavelength observed in  $S'$  and  $\lambda$  is the corresponding apparent wavelength observed in  $S$  and they are related by

$$\lambda = \frac{1 - \beta(\mathbf{v} \cdot \mathbf{V}/|\mathbf{v}\|\|\mathbf{V}\|)}{\sqrt{1 - \beta^2}} \lambda'. \quad (40)$$

Doppler effect states the difference of photon energy between reference frames. Since photon energy  $E_{\text{photon}} = h\nu = hc/\lambda$  is inversely proportional to wavelength, all the differences in photon energy can attribute to spectral shift.

## 5. SCENE IRRADIANCE AND SHADOWS

Two problems are discussed in this section: (1) how to determine the incident irradiance at a scene point coming from a moving light source; and (2) how to generate shadows. Let's first consider the first problem. Let  $P_l$  be a point light source with uniform radiant intensity  $I_l$  (watts per steradian), and let  $S''$  be the rest coordinate system of  $P_l$ , which is moving with velocity  $\mathbf{v}_l = (v_{lx}, v_{ly}, v_{lz})$  relative to the object rest coordinate system  $S'$ . As shown in Figure 7, let  $P'_{obj}(x'_{obj}, y'_{obj}, z'_{obj})_{S'}$  be a scene point on the object, and we want to determine the incident irradiance at  $P'_{obj}$  due to  $P_l$  at time  $t' = t'_{obj}$ .

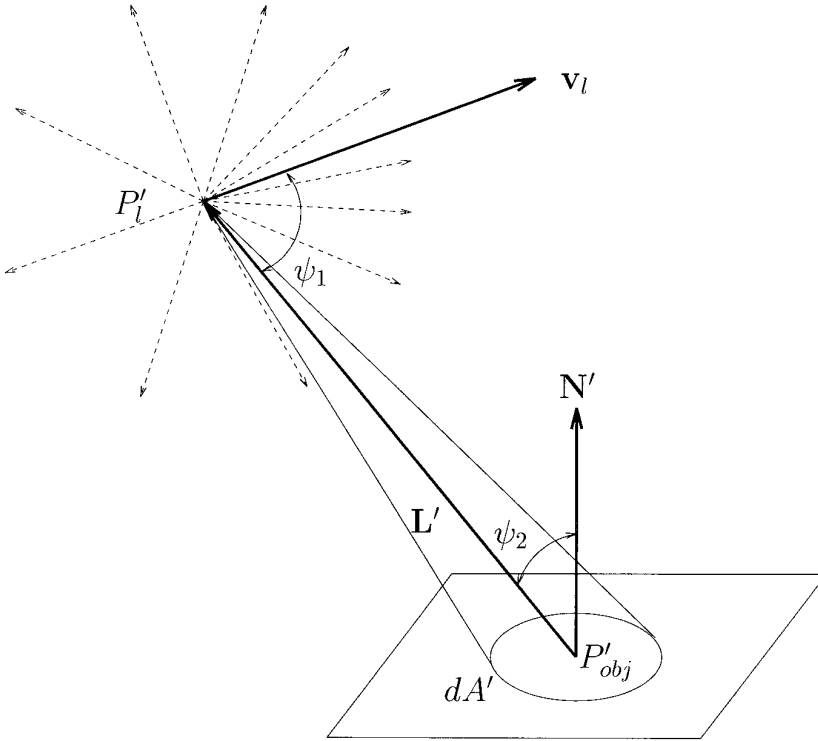


Fig. 7. Determining the incident irradiance at the scene point  $P'_{obj}$  coming from a moving light source  $P_l$ .  $P'_l$  is the apparent position of  $P_l$  w.r.t.  $P'_{obj}$  at time  $t' = t'_{obj}$ .

The Lorentz transformation connecting the space-time coordinates  $(x', y', z', t')_{S'}$  and  $(x'', y'', z'', t'')_{S''}$  for the same event can be expressed as

$$\begin{pmatrix} x' \\ y' \\ z' \\ t' \end{pmatrix} = \begin{pmatrix} L_{11}(\mathbf{v}_l) & L_{12}(\mathbf{v}_l) & L_{13}(\mathbf{v}_l) & L_{14}(\mathbf{v}_l) \\ L_{21}(\mathbf{v}_l) & L_{22}(\mathbf{v}_l) & L_{23}(\mathbf{v}_l) & L_{24}(\mathbf{v}_l) \\ L_{31}(\mathbf{v}_l) & L_{32}(\mathbf{v}_l) & L_{33}(\mathbf{v}_l) & L_{34}(\mathbf{v}_l) \\ L_{41}(\mathbf{v}_l) & L_{42}(\mathbf{v}_l) & L_{43}(\mathbf{v}_l) & L_{44}(\mathbf{v}_l) \end{pmatrix} \begin{pmatrix} x'' \\ y'' \\ z'' \\ t'' \end{pmatrix}. \quad (41)$$

Suppose the light source  $P_l$  is at rest at  $(x''_{l0}, y''_{l0}, z''_{l0})_{S''}$  in its coordinate system  $S''$ , then the motion equation for  $P_l$  with respect to the object rest coordinate system  $S'$  can be described as

$$x'_l = x'_{l0} + v_x t'_l, \quad (42)$$

$$y'_l = y'_{l0} + v_y t'_l,$$

$$z'_l = z'_{l0} + v_z t'_l,$$

where  $(x'_l, y'_l, z'_l)_{S'}$  is the position of  $P_l$  when time  $t' = t'_l$  and  $(x'_{l0}, y'_{l0}, z'_{l0})_{S'}$  is the position of  $P_l$  when time  $t' = t'_{l0}$ .

$z'_{l0})_{S'}$  is the position of  $P_l$  at  $t' = t'' = 0$ , that is,

$$\begin{aligned}x'_{l0} &= L_{11}(\mathbf{v}_l)x''_{l0} + L_{12}(\mathbf{v}_l)y''_{l0} + L_{13}(\mathbf{v}_l)z''_{l0}, \\y'_{l0} &= L_{21}(\mathbf{v}_l)x''_{l0} + L_{22}(\mathbf{v}_l)y''_{l0} + L_{23}(\mathbf{v}_l)z''_{l0}, \\z'_{l0} &= L_{31}(\mathbf{v}_l)x''_{l0} + L_{32}(\mathbf{v}_l)y''_{l0} + L_{33}(\mathbf{v}_l)z''_{l0}.\end{aligned}$$

To evaluate the action of  $P_l$  on  $P'_{obj}$  at time  $t' = t'_{obj}$ , we must take the propagation delay of light signals into account and find the apparent position of  $P_l$  with respect to  $P'_{obj}$  at time  $t' = t'_{obj}$ . The space coordinates  $(x'_l, y'_l, z'_l)_{S'}$  are regarded as the apparent position of  $P_l$  w.r.t.  $P'_{obj}$  at the instant  $t' = t'_{obj}$  if they satisfy the motion equation given in Eq. (42) and the following requirement:

$$(x'_l - x'_{obj})^2 + (y'_l - y'_{obj})^2 + (z'_l - z'_{obj})^2 = c^2(t'_{obj} - t'_l)^2, \quad t'_l < t'_{obj}. \quad (43)$$

Let  $(x'_{ll}, y'_{ll}, z'_{ll})$  be the solution for  $(x'_l, y'_l, z'_l)$  to Eqs. (42) and (43), and in Figure 7 we denote this apparent position as  $P'_l$ . Although the point light source  $P_l$  emits power uniformly in all directions in its own rest coordinate system  $S''$ , from the viewpoint of  $S'$  the apparent radiant intensity of  $P_l$ , denoted as  $I_a$ , is no longer isotropic because of the effect of aberration. As shown in Figure 7, let  $dA'$  be the area of a small planar patch centered at  $P'_{obj}$ , and let  $d\Omega'_{obj}$  be the solid angle subtended by  $dA'$ , as seen from  $P'_l(x'_{ll}, y'_{ll}, z'_{ll})_{S'}$ . According to the discussion in the previous section, from the viewpoint of the coordinate system  $S''$ , the solid angle subtended by  $dA'$ , denoted by  $d\Omega''_{obj}$ , might be different from  $d\Omega'_{obj}$ . Similar to Eq. (35), the relation between  $d\Omega'_{obj}$  and  $d\Omega''_{obj}$  is connected by

$$d\Omega''_{obj} = \frac{\sqrt{1 - \beta_l^2}}{1 - \beta_l \cos \psi_1} d\Omega'_{obj} = \frac{\sqrt{1 - \beta_l^2}}{1 + \beta_l(\mathbf{v}_l \cdot \mathbf{L}' / |\mathbf{v}_l| |\mathbf{L}'|)} d\Omega'_{obj}, \quad (44)$$

where  $\beta_l = \|\mathbf{v}_l\|/c$  and

$$\mathbf{L}' = (x'_{ll} - x'_{obj}, \quad y'_{ll} - y'_{obj}, \quad z'_{ll} - z'_{obj}). \quad (45)$$

Since for the same amount of power the radiant intensity is inversely proportional to the solid angle the power flows through, the apparent radiant intensity  $I_a$  can be expressed in terms of  $I_l$ :

$$I_a = \frac{d\Omega''_{obj}}{d\Omega'_{obj}} I_l = \frac{\sqrt{1 - \beta_l^2}}{1 + \beta_l(\mathbf{v}_l \cdot \mathbf{L}' / |\mathbf{v}_l| |\mathbf{L}'|)} I_l.$$

$d\Omega'_{obj}$  can be written as

$$d\Omega'_{obj} = \frac{\cos \psi_2 \cdot dA'}{|\mathbf{L}'|^2} = \frac{\mathbf{L}' \cdot \mathbf{N}' / |\mathbf{L}'| |\mathbf{N}'|}{|\mathbf{L}'|^2} dA'.$$

The power originating from  $P'_l$  passing the solid angle  $d\Omega'_{obj}$ ,  $d\varphi_l$ , can be obtained by multiplying the apparent radiant intensity with the solid angle  $d\Omega'_{obj}$ :

$$\begin{aligned} d\varphi_l &= \frac{\sqrt{1 - \beta_l^2}}{1 + \beta_l(\mathbf{v}_l \cdot \mathbf{L}' / |\mathbf{v}_l| |\mathbf{L}'|)} I_l \cdot d\Omega'_{obj} \\ &= \frac{\sqrt{1 - \beta_l^2}}{1 + \beta_l(\mathbf{v}_l \cdot \mathbf{L}' / |\mathbf{v}_l| |\mathbf{L}'|)} \frac{\mathbf{L}' \cdot \mathbf{N}' / |\mathbf{L}'| |\mathbf{N}'|}{|\mathbf{L}'|^2} I_l dA'. \end{aligned}$$

Divide  $d\varphi_l$  by  $dA'$  and we can obtain the incident irradiance at  $P'_{obj}$  coming from the point light source  $P'_l$ :

$$\mathcal{J}^{i'}(\mathbf{L}'(P_l)) = \frac{d\varphi_l}{dA'} = \frac{\sqrt{1 - \beta_l^2}}{1 + \beta_l(\mathbf{v}_l \cdot \mathbf{L}' / |\mathbf{v}_l| |\mathbf{L}'|)} \frac{\mathbf{L}' \cdot \mathbf{N}' / |\mathbf{L}'| |\mathbf{N}'|}{|\mathbf{L}'|^2} I_l. \quad (46)$$

Again, if the Doppler effect is taken into account,  $\mathcal{J}^{i'}(\mathbf{L}'(P_l))$  and  $I_l$  must be expressed as spectral energy distribution functions of wavelength and the above equation can be written as

$$\mathcal{J}^{i'}(\mathbf{L}'(P_l); \lambda') = \frac{\sqrt{1 - \beta_l^2}}{1 + \beta_l \mathbf{v}_l \cdot \mathbf{L}' / |\mathbf{v}_l| |\mathbf{L}'|} \frac{\mathbf{L}' \cdot \mathbf{N}' / |\mathbf{L}'| |\mathbf{N}'|}{|\mathbf{L}'|^2} I_l(\lambda''), \quad (47)$$

where  $\lambda''$  is the observed wavelength observed in  $S''$  and  $\lambda'$  is the corresponding apparent wavelength observed in  $S'$ , that is,

$$\lambda' = \lambda'' \frac{1 + \beta_l(\mathbf{v}_l \cdot \mathbf{L}' / |\mathbf{v}_l| |\mathbf{L}'|)}{\sqrt{1 - \beta_l^2}}. \quad (48)$$

So far, we have assumed that the light beams emitted from the light sources will arrive at the scene points without blocking. However, objects may cast shadows on one another. When the relativistic effects are taken into account, the generation of shadows is more complicated and time-consuming than it is in traditional computer graphics, because now the propagation delay of light signals is no longer negligible and this prevents the application of some traditional shadow algorithms, such as scan-line generation [Appel 1968; Bouknight and Kelly 1970], shadow volumes [Crow 1977], shadow polygons [Atherton et al. 1978], and shadow z-buffer [Williams 1978]. Let's take the shadow z-buffer algorithm as an example to show why those algorithms fail. The shadow z-buffer algorithm is a two-step process. In the first step, a scene is 'rendered' (in fact, no intensities are calculated) and depth information is stored into the shadow z-buffer taking the light source as a view point. This step computes a 'depth image' from the light source, of those polygons visible to the light source.

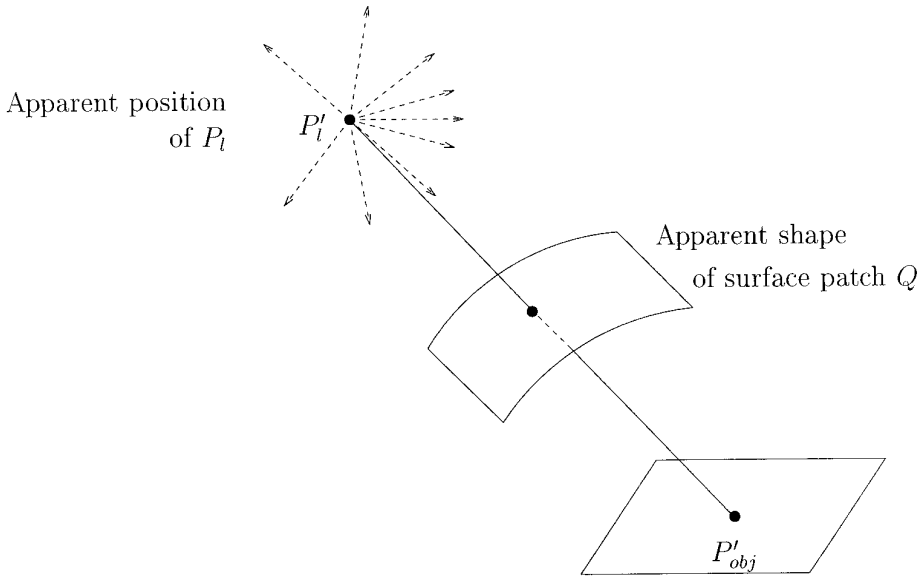


Fig. 8. Determining whether the scene point  $P'_{obj}$  is illuminated by the light source  $P_l$ .

The second step is to render the scene for the real view point with the shadow information contained in the depth images. Notice that the shadow information in a depth image is valid only with respect to the corresponding light source at some instant, say,  $t'' = t'_l$ . However, since it generally takes different amounts of time for the photons emitted from the light source to travel to the various points on the object, reflect on the surface of the object, and reach the viewer, the shadow information is generally useless for the real view point unless there is no relativistic relative motion between the light source, the scene, and the viewer.

Figure 8 shows how to determine shadows correctly. Let  $P_l$  and  $P'_{obj}$  denote the light source and the scene point mentioned above, and let  $Q$  denote a surface patch, which is moving relative to the scene point  $P'_{obj}$ . We want to determine whether the light beam from  $P_l$  to  $P'_{obj}$  is blocked by the surface patch  $Q$ . As before, the apparent position of  $P_l$  w.r.t.  $P'_{obj}$  at  $t' = t'_{obj}$ , denoted by  $P'_l$  in Figure 8, is first found. From the viewpoint of  $P'_{obj}$ , the light beam from  $P_l$  propagates along the line segment  $\overline{P'_l P'_{obj}}$ , and if not blocked, will arrive at  $P'_{obj}$  at  $t' = t'_{obj}$ . Hence, the problem of determining whether  $Q$  will cast shadow on  $P'_{obj}$  at  $t' = t'_{obj}$  is equivalent to that of determining whether  $\overline{P'_l P'_{obj}}$  intersects with the apparent shape of  $Q$  w.r.t.  $P'_{obj}$  at  $t' = t'_{obj}$ , because the light beam will be blocked at the intersection point if there exists an intersection.

Since with different scene points the apparent position of  $P_l$  and the apparent shape of  $Q$  might be different, the process of generating shadows might be very time-consuming. Hence, shadows may be considered only when more realistic image and additional depth cues are pursued.

## 6. EXAMPLES

The shading process is summarized as follows:

- (1) Find the apparent shape of the object with respect to the viewer  $O$  who sees or photographs the object at time  $t = t_s$ .
- (2) For each point  $P_{obj}(x_{obj}, y_{obj}, z_{obj})_S$  on the surface of the apparent shape:
  - (a) Determine whether  $P_{obj}(x_{obj}, y_{obj}, z_{obj})_S$  is visible. If it is invisible, skip the following steps.
  - (b) Determine the viewing direction vector  $\mathbf{V}$  for  $P_{obj}(x_{obj}, y_{obj}, z_{obj})_S$  by Eq. (19).
  - (c) Determine the space-time coordinate  $(x'_{obj}, y'_{obj}, z'_{obj}, t'_{obj})$  by Eq. (8).  $(x'_{obj}, y'_{obj}, z'_{obj}, t'_{obj})_{S'}$  represent the position and time in the object rest coordinate system  $S'$ , that the scene point  $P'_{obj}, (x'_{obj}, y'_{obj}, z'_{obj})_{S'}$  emits the photons which arrive at the viewer  $O$  at time  $t = t_s$ .
  - (d) For each light source  $P_l$  (with radiant intensity  $I_l(\lambda'')$ ):
    - (i) Find the apparent position of  $P_l$  with respect to  $P'_{obj}(x'_{obj}, y'_{obj}, z'_{obj})_{S'}$  at time  $t' = t'_{obj}$ . Let the apparent position be denoted as  $P'_l$ .
    - (ii) Determine the light direction vector  $\mathbf{L}'$  for  $P'_l$  by Eq. (45).
    - (iii) Determine whether the light coming from  $P'_l$  is blocked from the scene point  $P'_{obj}(x'_{obj}, y'_{obj}, z'_{obj})_{S'}$ .
    - (iv) If the light coming from  $P'_l$  is not blocked from  $P'_{obj}$ , determine the incident irradiance  $J^{i'}(\mathbf{L}'(P_l); \lambda')$  coming from the light source  $P_l$  by Eqs. (47) and (48). If the light from  $P'_l$  is blocked from  $P'_{obj}$ ,  $J^{i'}(\mathbf{L}'(P_l); \lambda')$  is set to 0.
  - (e) Find the reflected radiance at  $P'_{obj}$  in the direction  $\mathbf{V}'$  in the object rest system  $S'$ ,  $J^{r'}(\mathbf{V}'; \lambda')$ . That is,

$$J^{r'}(\mathbf{V}'; \lambda') = \sum_{\text{all light source } P_l} BRDF(\mathbf{L}', \mathbf{V}'; \lambda') \cdot J^{i'}(\mathbf{L}'(P_l); \lambda').$$

- (f) Find the apparent scene radiance at  $P_{obj}(x_{obj}, y_{obj}, z_{obj})_S$  with respect to the viewer  $O$  at time  $t = t_s$ ,  $J^r(\mathbf{V}; \lambda)$ , by Eqs. (39) and (40).

Three examples showing the visual appearance of objects in relativistic motion are given in Figure 9. In the following, we always take the  $x$ -axis to be horizontally oriented, pointing to the right, the  $y$ -axis to be vertically oriented, pointing above, and the  $z$ -axis to be pointing out of the paper. Also, planar geometric projection is adopted, and the projection is obtained with respect to the  $z$ -axis. Figures 9(a), (c), and (e) show the original shapes of the illustrating objects, including a teapot, two cubes, and a sphere, when viewed in their own rest system  $S'$ . All the objects are moving relative to the viewer  $O$  with velocity  $\mathbf{v} = (0.95c, 0, 0)$ ; that is, they are moving in the direction of the  $x$ -axis. Figures 9(b), (d), and (f) show the snapshots of the objects taken by the viewer  $O$  when the central point of

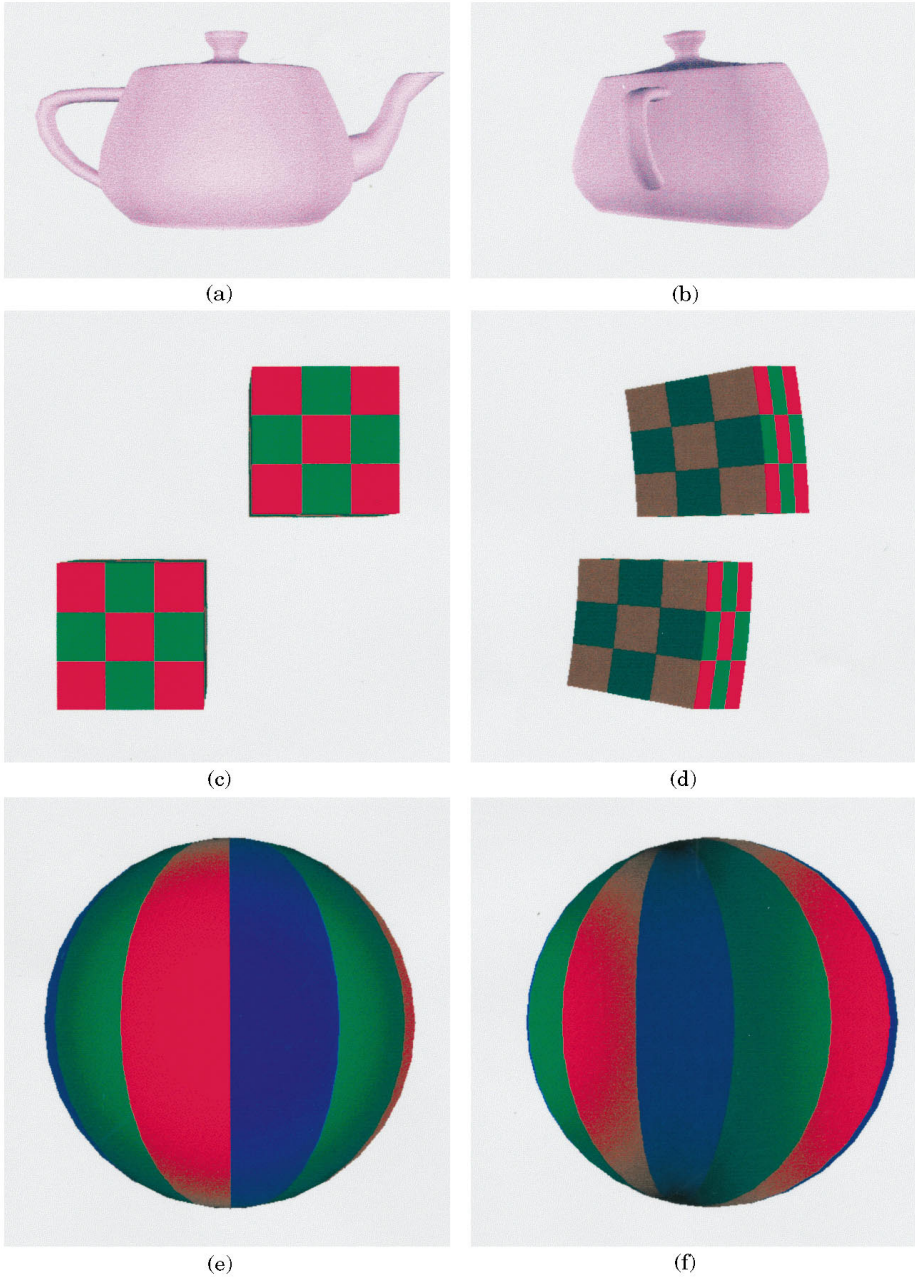


Fig. 9. The visual appearances of objects moving at relativistic speeds. All the objects in the examples are moving relative to the viewer  $O$  with velocity  $\mathbf{v} = (0.95c, 0, 0)$ . The left images (a), (c), (e) show the original shapes of the objects. The right images (b), (d), (f) show the visual appearances of the objects for the viewer  $O$ .

the object appears at the center of the projection plane (that is, when the viewing direction vector for the center of object makes a right angle with the direction of motion). If the relativistic effects were negligible, the pictures in Figures 9(b), (d), and (f) should be the same as those in Figures 9(a), (c), and (e), respectively. From these examples, we see obvious distortion in the appearance of rapidly moving objects. For example, the spout of the teapot keeps pointing in the direction of the positive  $x$ -axis during the motion, but there is an obvious rotation of the teapot around the  $y$ -axis in Figure 9(b), and the spout of the teapot becomes invisible. Moreover, we see that one side of the teapot has swollen and the other side has shrunk, and the symmetric axis of the body of the teapot has bent. From Figure 9(d), a similar effect of rotation can be observed: the faces with plane normals originally pointing in the direction of the  $z$ -axis have foreshortened and the faces with plane normals pointing in the direction of the negative  $x$ -axis have become more exposed. Moreover, the edges of the cubes originally parallel to the  $y$ -axis have bent. For the example of the sphere, a similar effect of rotation and distortion is also observed. Surprisingly, although part of the sphere has swollen and part of it has shrunk, a rapidly moving sphere still has a circular outline, which Boas had proven by mathematical approach in his paper [Boas 1961].

Figure 10 shows a series of snapshots of the teapot when it is moving from left to right. The spout of the teapot always points to the right during the motion, and the successive snapshots are taken by the viewer  $O$  at the same time intervals. Notice that although the teapot is moving at constant speed, the viewer feels that it is moving at varying speed; the speed is reducing during the motion. From this example, we also see that when the teapot moves at a higher speed, the effect of rotation and distortion is more obvious. As shown in Figure 10(c), where the speed of the teapot is  $0.999c$ , even though the teapot is still approaching the viewer, only the rear side (the face with the handle) of the teapot is visible while the front face is invisible.

Figures 11 and 12 show the apparent appearance of more complex scenes, the STREET, including a street with buildings on both sides. Figure 11 shows the original shape of the STREET, and Figures 12(a) and (b) show the visual appearance of the STREET when the viewer rushes into the street and rushes out of the street at a speed of  $0.99c$ . From Figure 12(a), we first observe that both buildings have rotated. The right building has rotated around the  $y$ -axis, and the left building around the negative  $y$ -axis. This effect makes the front faces of the buildings (the faces with plane normal originally pointing in the direction of the  $z$ -axis) invisible, and the side faces of the buildings more exposed. Especially near the upper left corner of the picture, the back face of the tower of the left building, which is originally invisible, becomes visible. Next we observe that the buildings have bent to the center of the scenes in the longitudinal direction. This effect is more obvious for the scene points whose projectors make a larger angle with the  $z$ -axis. On the other hand, from Figure 12(b), it is found that when the viewer is moving rapidly away from the scenes the picture will

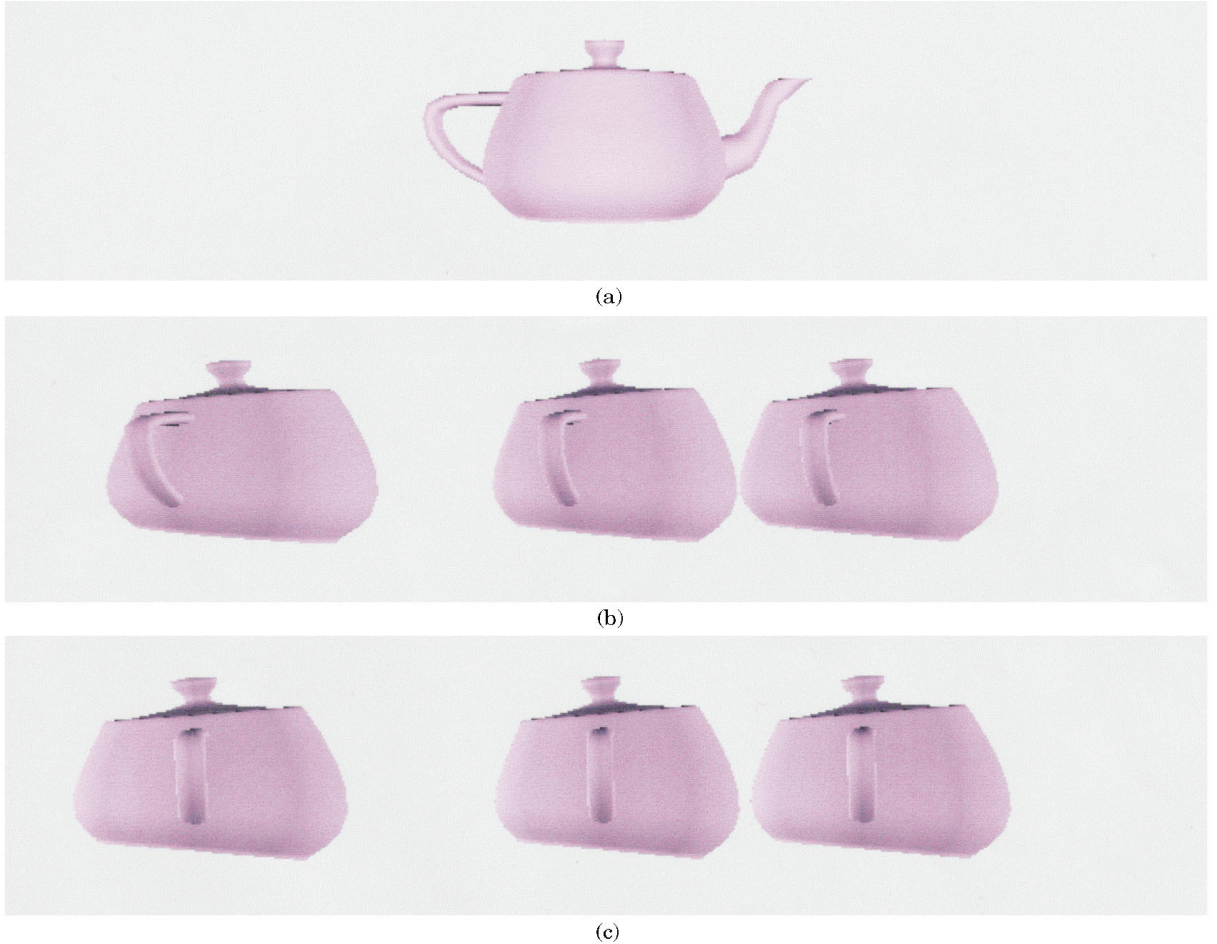


Fig. 10. Visual appearance of a moving teapot. (a) The teapot is still relative to the viewer. (b) The teapot is moving from the left to the right with a speed of  $0.95c$ . (c) The teapot is moving from the left to the right with a speed of  $0.999c$ .

look like the orthographic projection of the original scenes. That is because the angle that a light beam from the scenes makes with the  $z$ -axis is amplified in the coordinate system  $S$  such that only those light beams which originally make a tiny angle with the  $z$ -axis can reach the viewer.

Figure 13 shows the effect of radiance variation due to the motion of the scenes. In the example, there are three distant light sources which illuminate the teapot with light direction vectors  $(0, 0, 1)$ ,  $(1, 0, -1)$ , and  $(-1, 0, -1)$ , respectively, and the light sources are at rest in the coordinate system of the teapot. Compare this picture with that in Figure 10(b), where the effect of radiance variation is neglected. From Figure 13 we find that the teapot is brighter when it is at the left side of the viewer, and it grows darker and darker during its motion. That is because the angle that the viewing vector (from the teapot to the viewer) makes with the direction of



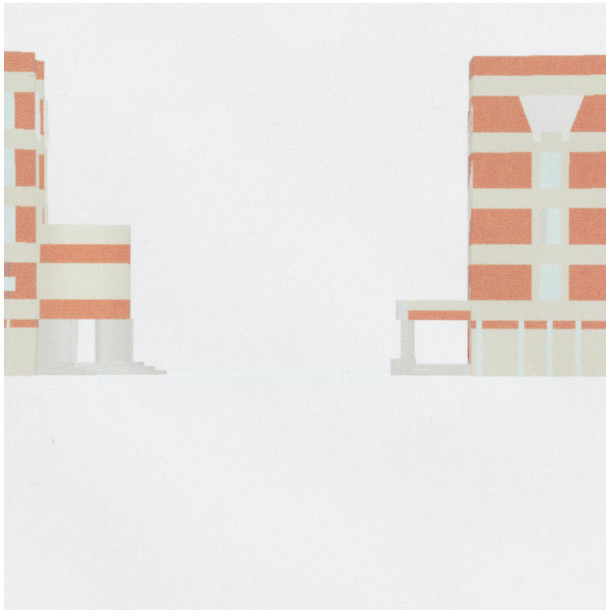
Fig. 11. Original appearance of the STREET.

motion becomes larger and larger during the motion. Figure 14 shows the STREET taking into account the effect of radiance variation. When the viewer is running into the street rapidly, he sees an image whose brightness is enhanced near the center. On the other hand, when the viewer is running away from the street rapidly, he sees an image whose brightness is reduced.

Figure 15(a) shows the effect due to the motion of light sources. Again, the teapot is moving relative to the viewer with a velocity of  $(0.95c, 0, 0)$ , but now the light sources are at rest in the coordinate system of the viewer (that is, there is a relative motion between the teapot and the light sources). Notice how different the pictures in Figure 15(a) and Figure 13 look just owing to a change in the velocity of the light sources. The motion of light sources causes a variation in the incident irradiance at the teapot, and this effect is shown in Figure 15(b), where the snapshot is taken by another viewer at rest in the coordinate system of the teapot. From the viewpoint of the teapot the light sources are moving with a velocity of  $(-0.95c, 0, 0)$ , and this makes the front side of the teapot get more irradiance from the light sources than the rear side. Hence, the picture in Figure 15(a) is a result of the mixed effects of scene radiance and irradiance variation, the relative motion between the light sources and the teapot causes the rear side of the teapot to be darker than the front side and the



(a)



(b)

Fig. 12. Apparent appearance of the STREET with respect to a moving viewer. (a) The viewer is rushing into the street with a speed of  $0.99c$ . (b) The viewer is rushing out of the street with a speed of  $0.99c$ .

relative motion between the teapot and the viewer causes the teapot to become darker and darker during its motion. Figure 16 gives another example, the STREET, showing the effect due to the motion of the light

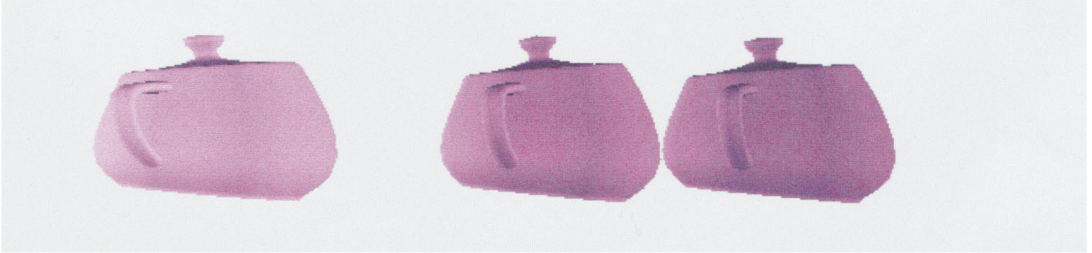


Fig. 13. Effect of scene radiance variation due to motion. The teapot is moving relative to the viewer from the left to the right with a speed of  $0.95c$ . The light sources are at rest in the coordinate system of the teapot.

source. All the conditions in Figures 16 and 14(a) are the same except the velocity of the light sources, but the appearances of the STREET in Figures 16 and 14(a) are quite different.

Figure 17 shows the Doppler effect. Here we have assumed that the surface of the teapot reflects light only at three narrow wavelength intervals around 460, 540, and 600 nanometers with different reflectivities, and the spectral energy distributions of the light sources are uniform over the spectral space (For the case of general spectral reflectance functions, spectral sampling like that in Hall and Greenberg [1983] is required for color calculations). The original color of the teapot is the same as that shown in Figure 9(a). From Figure 17, where the teapot is moving with a velocity of  $(0.5c, 0, 0)$  relative to the viewer, we see that the teapot has a color with shorter dominant wavelength when it is approaching the viewer and has a color with longer dominant wavelength when it is departing from the viewer. That is because the angle that the viewing vector (from the teapot to the viewer) makes with the direction of motion becomes larger and larger during the motion.

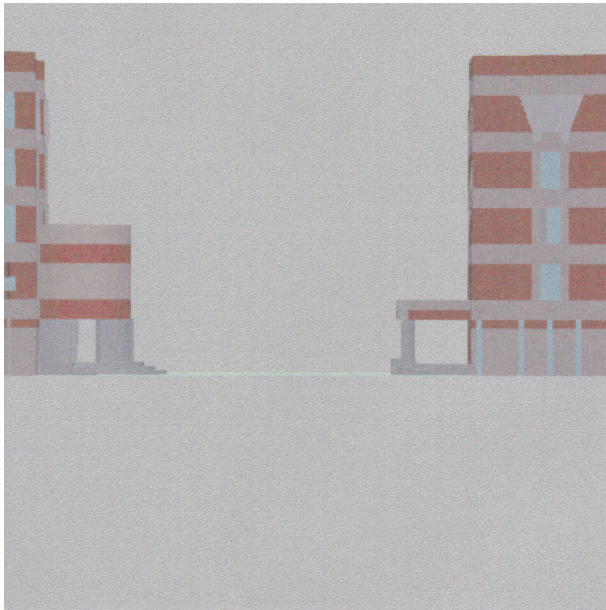
Figure 18 shows the unusual appearance of shadows under relativistic conditions. In this example there is a sphere, a floor, and a point light source. Both the floor and the light source are motionless relative to the viewer, and the light source is a great distance from the floor, with a light direction vector of  $(0, 1, 0)$  with respect to the floor. In Figure 18(a), where the sphere is at rest above the floor, its shadow has a circular outline, just as expected. However, as shown in Figure 18(b), when the sphere is moving with a velocity of  $(0.95c, 0, 0)$  relative to the viewer, its shadow is lengthened in the direction of motion and is lagging behind such that the viewer has the illusion that the light direction vector has changed.

## 7. RELATED WORK

In the papers by Hsiung [1990], Hsiung and Dunn [1989], Hsiung and Thibadeau [1990], and Hsiung et al. [1990d], a relativistic ray-tracer exploring the special-relativistic effects in graphics is implemented. Hsiung coined the term *REST-frame* for his method of rendering, based on the Lorentz transformation of light rays between the two coordinate systems  $S$



(a)



(b)

Fig. 14. Effect of scene radiance variation due to motion. (a) The viewer is rushing into the street with a speed of  $0.99c$ . (b) The viewer is rushing out of the street with a speed of  $0.99c$ . The light sources are at rest in the coordinate system of the street.

and  $S'$ , as defined in Section 3. A ray is a single space-time event. The Lorentz transformation is applied on rays fired from camera frame  $S$ , and the hit times of the transformed rays in the object frame  $S'$  are calculated

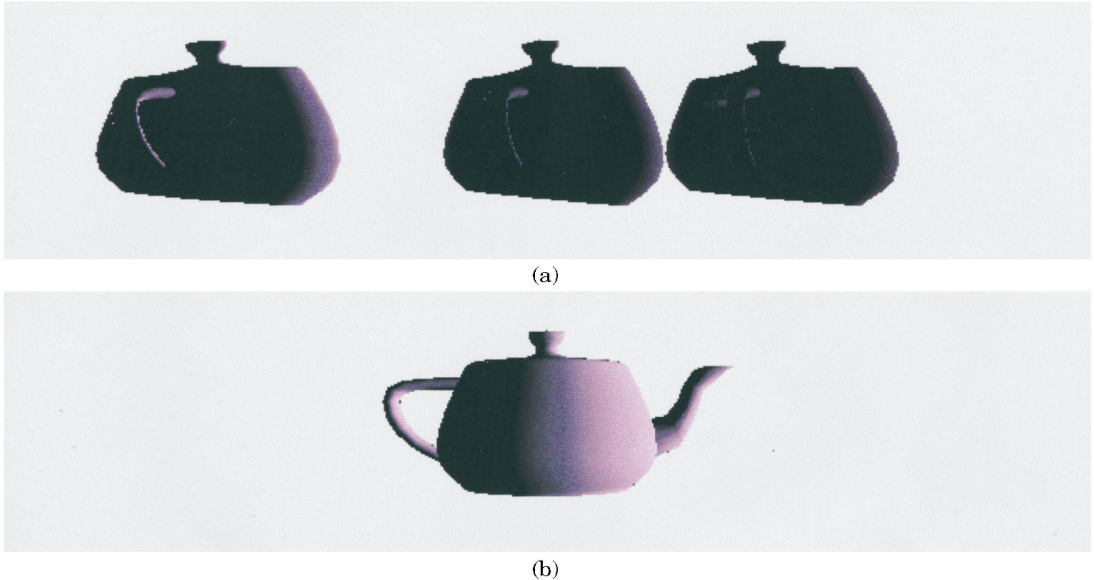


Fig. 15. Effects produced by the motion of light sources. (a) The teapot is moving relative to the viewer with a velocity of  $(0.95c, 0, 0)$ , and the light sources are at rest in the coordinate system of the viewer. (b) The light sources are moving relative to the teapot with a velocity of  $(-0.95c, 0, 0)$ , and the viewer is still relative to the teapot.

[Hsiung et al. 1990b]. Further reflected and refracted rays are generated from the hit events in  $S'$ , and the hit times for these generated rays in frame  $S'$  are calculated recursively. Multiple frames moving at different speeds relative to the camera frame  $S$  can also be processed by the extension of the *REST-frame* method. The reflected and refracted rays between different object frames can recursively reach other frames by applying Lorentz transformation and calculating the hit times of the rays. Light sources can be handled by adding shadow rays at hit events. Light sources moving at various speeds related to the viewer's frame  $S$  can be processed by finding one frame in which the light source is static. The Doppler effect is accounted for by adopting approximate spectrum for visible light, implemented by matrices. The resulting shifted spectrum is then converted into the RGB color system to comply with common raster display systems [Hsiung et al. 1990a; 1990c]. Since the ray-tracing technique is inherently too slow for most real-time interactive systems, the *T-buffer* approach is proposed [Hsiung et al. 1990e]. The *T-buffer* is similar to the conventional *Z-buffer*, except the *time* is stored in the buffer instead of the *depth*. Rays are fired from the camera frame and are transformed onto object frames. In this scheme, no recursive reflected or refracted rays are generated. The resulting color of a certain pixel is determined by the event with least delay time observed in the  $S$  frame. In the *T-buffer* scheme, however, the spatial reflection and refraction effects are not presented.

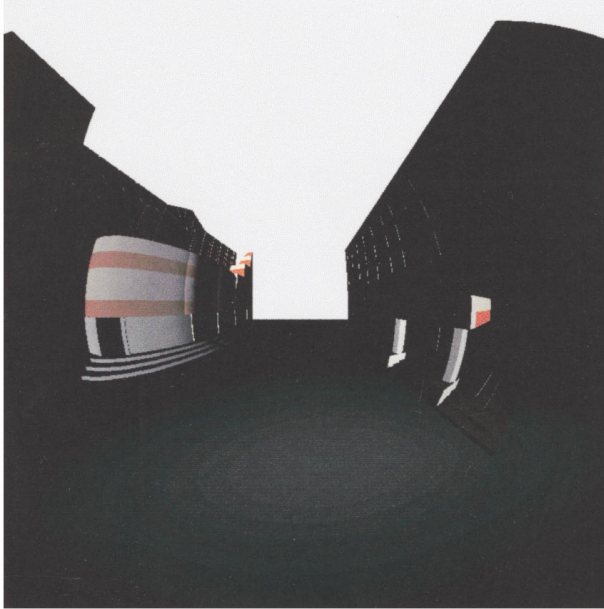


Fig. 16. Effects produced by the motion of light sources. All the conditions are the same as those in Figure 14(a), except that now the light sources are at rest in the coordinate system of the viewer.



Fig. 17. Variation in color due to the Doppler effect. The teapot is moving from the left to the right with a speed of  $0.5c$ , and the light sources are at rest in the coordinate system of the teapot.

The techniques used in Hsiung's paper are different from our work. We use a generic *bidirectional reflectance distribution function*  $BRDF(\theta_r, \phi_r, \theta_i, \phi_i)$  for the derivation; thus, every surface model can be readily substituted into the  $BRDF(\theta_r, \phi_r, \theta_i, \phi_i)$ , and all the effects in the original non-relativistic model can be retained with special relativity taken into account, with the overhead of Lorentz transformation matrix multiplication Eq. (41). Some surface models depend on wavelength; for example, Fresnel's equation in the Torrance-Sparrow model is wavelength-dependent. For such models, Eqs. (39) and (40) can be applied to take the Doppler effect into account. Wavelength-dependent models can further apply Eqs. (47)

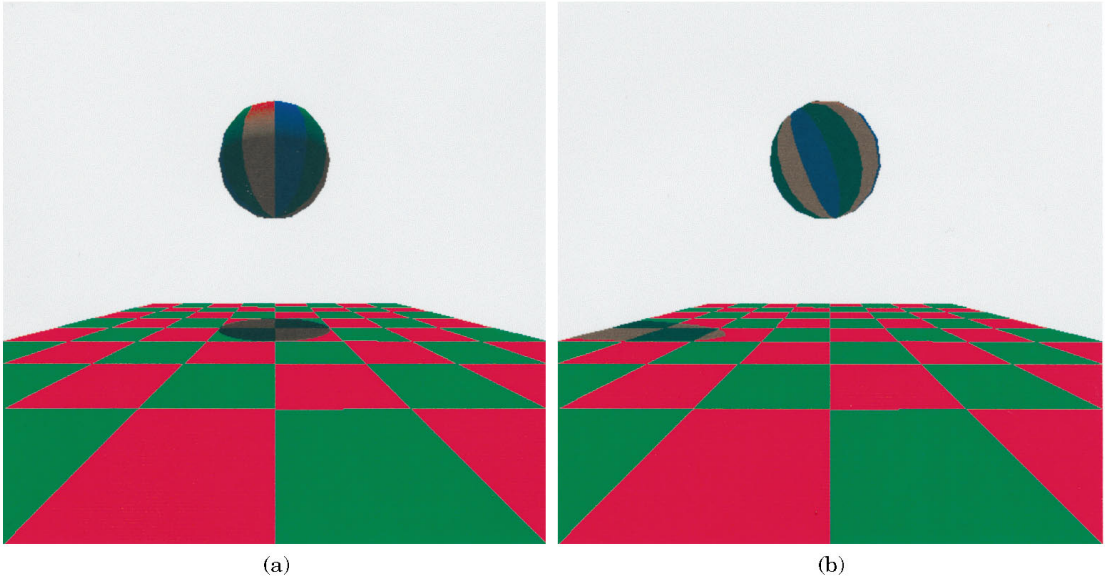


Fig. 18. Effect of generating shadows with the relativistic effects taken into account. (a) The sphere is still relative to the viewer. (b) The sphere is moving with a velocity of  $(0.95c, 0, 0)$  with respect to the viewer.

and (48) to include light sources moving relative to the objects. The rendering pipeline is essentially the same as the conventional non-relativistic approach, thus our methodology is especially suitable for interactive applications based on current systems. Shadows are also considered, although at a cost of significant additional computation. Our work, however, does not take refraction effects into account. To generate complicated scenes with shadows and refraction effects, we recommend ray-tracing methods such as Hsiung's.

We believe our goal of design is quite practical. All the current existing surface models or shading methods can be readily applied, with barely any performance penalty. By applying our methodology, an interactive relativistic environment can be constructed.

## 8. CONCLUSION

We have shown how to determine the visual appearance, apparent brightness, and apparent color for a rapidly moving object, and we have also shown how to generate shadows. Some important results are: (1) If an object is moving rapidly relative to the viewer, the viewer will get a rotated and distorted picture of the object, and the effect of rotation and distortion is more obvious as the relative speed increases; (2) Even though the object keeps moving at a constant speed, the viewer feels that it is moving at varying speeds; (3) If the light sources are at rest in the object rest coordinate system, the moving object will have a brighter appearance when it is approaching the viewer and a darker appearance when it is departing from the viewer; (4) If the light sources are at rest in the object rest

coordinate system, the moving object will have a color with a shorter dominant wavelength when it is approaching the viewer and will have a color with a longer dominant wavelength when it is departing from the viewer; (5) If the light sources are not fixed in the object rest coordinate system, the apparent brightness of the object reflects the mixed effects of irradiance variation and radiance variation. Moreover, a dramatic change in the apparent brightness may occur just owing to a change in the velocities of the light sources, as shown in Figures 15 and 16; (6) To determine whether one object may cast shadow on another object, the apparent positions of the light sources and the apparent shape of the first object with respect to the second object must be found.

Although in our daily lives we do not directly experience relativistic phenomena, the results can be applied in virtual environments and for entertainment and educational purposes in the future.

#### ACKNOWLEDGMENTS

We thank R. H. Thibadeau for providing us with invaluable reference materials during the revision of this paper.

#### REFERENCES

- APPEL, A. 1968. Some techniques for shading machine renderings of solids. *SIJJ*, 37–45.
- ATHERTON, P. R., WEILER, K., AND GREENBERG, D. 1978. Polygon shadow generation. *SIGGRAPH 78*, ACM, New York, 275–281.
- BOAS, M. L. 1961. Apparent shapes of large objects at relativistic speeds. *Am. J. Phys.* 29, 5 (May), 283–286.
- BOUKNIGHT, W. J., AND KELLY, K. C. 1970. An algorithm for producing half-tone computer graphics presentations with shadows and movable light sources. *Proceedings of the AFIPS, Spring Joint Computer Conference*, 1–10.
- CROW, E. C. 1977. Shadow algorithms for computer graphics. *SIGGRAPH 77*, ACM, New York, 242–247.
- HALL, R. A., AND GREENBERG, D. P. 1983. A testbed for realistic image synthesis. *IEEE CG & A 3*, 8 (Nov.), 10–20.
- HSIUNG, P. K. 1990. Visualizing relativistic effects. Ph.D. thesis, Department of Electrical and Computer Engineering, Carnegie Mellon Univ., Pittsburgh, Penn.
- HSIUNG, P. K., AND DUNN, R. H. P. 1989. Visualizing relativistic effects in spacetime. *Proceedings of Supercomputing '89 Conference*, 597–606.
- HSIUNG, P. K., AND THIBADEAU, R. H. 1990. Spacetime visualization of relativistic effects. *Proceedings of the 1990 ACM Eighteenth Annual Computer Science Conference*, Washington, DC, (Feb), ACM, New York, 236–243.
- HSIUNG, P. K., THIBADEAU, R. H., COX, C. B., AND DUNN, R. H. P. 1990a. Doppler color shift in relativistic image synthesis. *Proceedings of the International Conference on Information Technology*, Tokyo, Japan, (Oct.), 369–377.
- HSIUNG, P. K., THIBADEAU, R. H., COX, C. B., AND DUNN, R. H. P. 1990b. Time dilation visualization in relativity. *Proceedings of Supercomputing '90 Conference*, (Nov.).
- HSIUNG, P. K., THIBADEAU, R. H., COX, C. B., DUNN, R. H. P., OLBRICH, P. A., AND WU, M. 1990c. Wide-band relativistic doppler effect visualization. *Proceedings of the Visualization '90 Conference*, (Oct.), 83–92.
- HSIUNG, P. K., THIBADEAU, R. H., AND DUNN, R. H. P. 1990d. Ray-tracing relativity. *Pixel*, (Jan./Feb.), 10–18.

- HSIUNG, P. K., THIBADEAU, R. H., AND WU, M. 1990e. T-buffer: fast visualization of relativistic effects in spacetime. *Proceedings of the 1990 Symposium on Interactive 3D Graphics*, 83–88.
- MØLLER, C. 1955. *The Theory of Relativity*. Oxford University Press, New York.
- SCOTT, G. D., AND VINER, M. R. 1965. The geometrical appearance of large objects moving at relativistic speeds. *Amer. J. Phys.* 33, 7 (July), 534–536.
- TERRELL, J. 1959. Invisibility of the Lorentz Contraction. *Phys. Rev.* 116, 4 (Nov.), 1041–1045.
- WEISSKOPF, V. F. 1960. The visual appearance of rapidly moving objects. *PT 13*, 24 (Sept.), AIP, Washington, D.C., 24–27.
- WILLIAMS, L. 1978. Casting curved shadows on curved surfaces. *SIGGRAPH 78*, ACM, New York, 270–274.

Received June 1994; revised October 1995; accepted May 1996